Recent Advances in Fermentative Production of C4 Diols and their Chemo-catalytic Upgrading to High-value Chemicals

Abhishek R Varma [a], Bhushan S. Shrirame [a], Sunil K. Maity [a]*, Deepti Agrawal [b], Naglis Malys [c], Leonardo Rios-Solis [d], Gopalakrishnan Kumar [e], Vinod Kumar [f, g, h]*

[a] Department of Chemical Engineering, Indian Institute of Technology Hyderabad, Kandi, Sangareddy-502284, Telangana, India

[b] Biochemistry and Biotechnology Area, Material Resource Efficiency Division, CSIR-Indian Institute of Petroleum, Dehradun-248005, Uttarakhand, India

[c] Department of Organic Chemistry, Faculty of Chemical Technology, Kaunas University of Technology, Radvilėnų Street 19, LT-50254 Kaunas, Lithuania

[d] Department of Biochemical Engineering, University College London, Gower Street, London WC1E 6BT, UK

[e] School of Civil and Environmental Engineering, Yonsei University, Seoul 03722, Republic of Korea

[f] School of Water, Energy and Environment, Cranfield University, Cranfield MK43 0AL, United Kingdom

[g] Department of Bioscience and Bioengineering, Indian Institute of Technology Roorkee, Uttarakhand 247667, India

[h] C-Source Renewables Limited, Summit House, 4 – 5 Mitchell Street, Edinburgh, EH6 7BD, UK

*Corresponding authors:

1. Sunil K. Maity, Phone: +91-40-23016202, E-mail: sunil_maity@che.iith.ac.in
2. Vinod Kumar, Phone: +44 (0) 1234754786, E-mail: Vinod.Kumar@cranfield.ac.uk

Abstract

Non-renewability, non-sustainability, and negative environmental impacts of petrochemicals inspired the scientific community to develop bio-renewable manufacturing processes. The current era is witnessing the transition from a fossil-dominated economy towards sustainable and low-carbon green manufacturing technologies at economical prices with reduced energy usage. The biological production of chemical building blocks from biomass using cell factories is a potential alternative to fossil-based synthesis. However, microbes have their own limitations in generating the whole spectrum of petrochemical products. Therefore, there is a growing interest in an integrated approach where products containing active functional groups obtained by biological upgrading of biomass are converted via chemo-catalytic routes. The present review focuses on the biological production of three important structural isomers of C4 diols, 2,3, 1,3, and 1,4-butanediol, which are currently manufactured from petroleum to meet the soaring global market demand. The review starts with justifications for the integrated approach and summarizes the current status of the biological production of these diols, including the substrates, microorganisms, metabolic/pathway engineering, and fermentation technology. This is followed by a comprehensive review of recent advances in catalytic upgrading of C4 diols to generate a range of products. The roles of various active sites in the catalyst on catalytic activity, product selectivity, and catalyst stability are discussed. The review also covers examples of integrated approaches, addresses challenges associated with developing end-to-end processes for bio-based production of C4 diols, and underlines existing limitations for their upgrading via direct catalytic conversion. Finally, the concluding remarks and prospects emphasise the need for an integrated biocatalytic and chemo-catalytic approach to broaden the spectrum of products from biomass.

Keywords: Butanediols; Fermentation; Metabolic Engineering; Heterogeneous Catalysis; 1,3-Butadiene; 3-Buten-1-ol; 3-Buten-2-ol; Methyl ethyl ketone

1. Introduction

Depleting fossil reserves and associated adverse environmental impacts demand the production of clean, green, and renewable chemicals from sustainable feedstocks. The situation has been worsened by the exponentially growing world population. Therefore, there is an urgent need for sustainable alternatives to petrochemicals. Biomass is an inexhaustible resource formed through atmospheric carbon capture. This alternative renewable feedstock is anticipated to meet increasingly growing demands for materials, energy, and chemicals [1–3]. The diverse chemical composition of biomass allows the development of novel manufacturing processes for producing several bio-based chemicals in an integrated biorefinery approach [4,5]. The transition from petrochemicals to bio-based products can significantly contribute to sustainability, simultaneously curbing carbon emissions [6]. In the last decade, tremendous efforts have been made to develop commercially competitive bio-based chemicals, triggered by the US Department of Energy (DoE), which identified a potential list of platform chemicals obtained from biomass in the year 2004 [7]. The market of bio-based products is continuously growing since then, and the total value is forecasted to reach ~$100 billion with a compound annual growth rate of 10.47% [8].

The efficient microbial biocatalysts play a pivotal role in transforming biomass into various products, including fuels, chemicals, polymers, etc. However, whole ranges of petrochemical products are not accumulated in high yields. For example, biotechnological production of C4 alcohol like *n*-butanol started a century ago, yet this process is struggling with techno-commercial viability due to low solvent titres, <20-30 g/L. The primary reason for such a low solvent titer is the high toxicity, which is attributed to the hydrophobicity of n-butanol. In contrast, C_4 diols have been amassed in very high titers (>100 g/L) due to the coexistence of two OH groups, making them highly polar, hygroscopic, soluble in water, and cell friendly [9,10]. Similarly, the accumulation of hydrocarbons is relatively low, less than a few g/L. This problem can be overcome by an integrated approach combining fermentation technology and chemo-catalytic conversion. For example, 1,3-butadiene (BD), which is otherwise difficult to obtain via microbial fermentation, can be produced through catalytic dehydration of biomass-derived butanediols (BDO) [11–13].

Butanediols ($C_4H_{10}O_2$) represent four structural isomers of straight-chain C4 diols (Table 1). Currently, BDOs are produced by the petrochemical route [14,15]. For instance, four technologies are used to produce 1,4-BDO from acetylene, propylene, butadiene, and butane [16–18]. However, the Reppe chemistry-based process, which involves ethynylation of formaldehyde, followed by 1,4-butynediol hydrogenation to 1,4-BDO, is the most dominating technology. Davy process includes esterification of maleic anhydride (obtained from oxidation of benzene or n-butane) followed by vapour phase hydrogenation, while the Mitsubishi process includes the three-steps catalytic reaction of BD and acetic acid to 1,4-diacetoxy-2-butene, followed by hydrogenation and hydrolysis to 1,4-diacetoxybutane, and 1,4-BDO, respectively. In the Toyo Soda method, BD is chlorinated to a mixture of 1,4-dichloro-2-butene and 3,4-dichloro-1-butene, which on treatment with sodium acetate, gives 1,4-diacetoxy-2-butene, followed by hydrogenation to 1,4-BDO. 2,3-BDO is produced from 2-butylene via an epoxide

3

intermediate [19]. 1,3-BDO is produced by aldol condensation of acetaldehyde, followed by hydrogenation of resulting 3-hydroxybutyraldehyde (3-HBAD). However, the present catalytic manufacturing of BDOs is associated with harsh conditions and high production prices. These factors prompted the biological production of BDOs. The global BDOs market reached approximately 3.3 million tons in 2022 and is anticipated to grow at a healthy compound annual growth rate of 4.38% for the forecasted period up to 2030 [20].

The diols, especially 2,3-, 1,4-, and 1,3-BDO, have received renewed interest owing to their vast derivative potentials due to the existence of two OH groups at different positions. These favorable features are exploited in various industrial sectors for manufacturing fuels, solvents, monomers, and pharmaceutical precursors from BDOs [14,15,21]. The environmentally benign green products have rekindled significant interest in sustainable low-carbon manufacturing technologies. In this regard, fermentation technology plays a vital role, which can switch human society away from fossil-based BDOs to sustainable technologies and mitigate the harms of chemical synthesis. Dedicated research efforts have been made to design microbial cell factories to produce BDOs at high titres, yield, and productivity (TYP). Fermentative production of 2,3-BDO started >100 years ago with many literature reports, while only a handful of studies are available on the production of 1,3-BDO and 1,4-BDO via microbial route [10,22,23].

The present review provides comprehensive and up-to-date information on the production of bio-based C4 diols, including the substrates, microorganisms, metabolic/pathway engineering, and fermentation technology. It further apprises on emerging trends in chemo-catalytic upgrading of BDOs to various valuable products in an elaborative manner. The knowledge of reaction mechanisms and catalyst active sites is critical for the successful conversion of BDOs to a desired product. The review thus focuses on the fundamental understanding of the reaction mechanism and impact of active sites on catalytic activity, product yield and selectivity, besides the activity and stability of catalysts. The review also covers examples of commercial initiatives, catalytic upgrading of fermentative BDOs, and challenges associated with the biological upgrading of sugars to BDOs and their catalytic conversion. Finally, the review includes concluding remarks, future directions, and opportunities with the argument for an integrated biocatalytic and chemo-catalytic approach to broaden the spectrum of bio-based products.

2. Fermentative production of butanediols

2.1. 2,3-Butanediol (2,3-BDO)

2,3-BDO is C_4 metabolite and exists in three stereoisomeric forms: levo (2R,3R), dextro (2S,3S), and meso (2R,3S) [24]. However, separating and purifying these stereoisomers is tedious in the petrochemical route [24]. Therefore, the microbial route has been developed for the cost-effective, green, and environmentally friendly production of 2,3-BDO [10]. 2,3-BDO has a multitude of applications in the chemical, food, and pharmaceutical industries. The estimated global market of 2,3-BDO and its downstream products is ~32 million tons annually, valued at $43 billion [25,26]. 2,3-BDO also has the potential to serve as a biofuel due to its high heating value

(27.2 kJ/g), which is comparable to ethanol (29 kJ/g). Besides, the high hygroscopicity makes storing and transporting 2,3-BDO more economical and safer than ethanol [9,24,27].

Biochemistry of microbes accumulating 2,3-BDO. Unlike 1,3-BDO and 1,4-BDO, 2,3-BDO is a natural product of microbial systems and has matured technologically in recent decades, as reflected by high production rates [8]. The native 2,3-BDO-producing microbes include *Klebsiella, Bacillus* species*, Serratia marcescens, Enterobacter aerogenes, Pseudomonas chlororaphis,* etc. The metabolic pathway for 2,3-BDO biosynthesis starts with self-condensation of two molecules of pyruvate to α-acetolactate, catalysed by α-acetolactate synthase (ALS; *budB*) with loss of one carbon atom as CO_2. This is followed by the decarboxylation of α-acetolactate to acetoin by α-acetolactate decarboxylase (*budA*) with the loss of another carbon atom. The keto group of acetoin is further hydrogenated by 2,3-butanediol dehydrogenase (BDH) or acetoin reductase (AC) (*budC*) using NADH as a reductant (Fig. 1). The stereospecificity of BDH/AC dictates the optical purity of 2,3-BDO, which can be manipulated by modulating the stereospecificity of BDH/AC in a host strain [24,28–30]. The pathway also generates diacetyl via non-enzymatic oxidative decarboxylation in the presence of oxygen, and the partial reduction of diacetyl results in acetoin by the action of diacetyl reductase. Altogether two moles of pyruvate are assembled into one mole of 2,3-BDO, which is accompanied by the loss of two moles of CO_2. The pyruvate is also diverted towards the formation of other undesirable products, including acetoin, ethanol, acetic, lactic, succinic, and formic acid, which is another reason for carbon loss. All these should be minimized to recover maximal carbon in the form of 2,3-BDO (Fig. 1) [24,31]. It has been hypothesized that the 2,3-BDO pathway is triggered to counteract the intracellular acidification by diversion of carbon flux towards neutral metabolite 2,3-BDO, NADH/NAD+ balance, and storing carbon for cell growth. The reversible conversion between acetoin and 2,3-BDO with concomitant NADH/NAD+ transformation contributes towards maintaining the intracellular NADH/NAD+ ratio [32,33]. In case of depletion of the primary carbon source, the accumulated 2,3-BDO can be used as the source of carbon and energy [24,34].

2,3-BDO accumulation from pure and crude renewable carbon sources. Many 2,3-BDO accumulating organisms, including bacteria and yeast strains, have been isolated and genetically engineered for high-level production. The microbes with the natural ability to accumulate 2,3-BDO can synthesize it from a variety of carbon sources, including sucrose, glucose, fructose, galactose, mannose, xylose, arabinose, and glycerol [24,31,35]. Table 2 summarises biosynthesis of 2,3-BDO from several pure substrates by various naturally producing bacterial strains and non-natural producer *Saccharomyces cerevisiae*. Among pure carbon sources, maximum 2,3-BDO production (100-160 g/L) has been achieved from glucose and sucrose as carbon sources. On the other hand, utilization of xylose and glycerol have resulted in comparatively low TYP metrics.

Like several other metabolites, the excessive manufacturing price of 2,3-BDO stems from the high cost of substrates and downstream processing, limiting the industrial viability of the bioproduction. This has led to a search for inexpensive renewable feedstocks. As a result, the last decade has witnessed several investigations employing cheap crude renewable sources, including apple pomace, corn stover, crude glycerol, cassava, inulin,

jerusalem artichoke, molasses, sugarcane bagasse, etc., for microbial synthesis of 2,3-BDO (Table 2). For instance, Narisetty et al. used bread waste, a major food waste in Europe & USA, for fermentative 2,3-BDO production by a random mutant strain of *Enterobacter ludwigii* [22]. The strain accumulated 138.8 g/L with a yield of 0.48 g/g and productivity of 1.45 g/L. h using sugar-rich hydrolysate from bread waste, and similar results were obtained on pure glucose (144.5 g/L, 0.47 g/g; 1.51 g/L. h). When the same strain was employed for testing cellulosic sugars from brewer's spent grains, it yielded 118.5 g/L 2,3-BDO using cellulosic sugars from brewer's spent grains [25]. However, titer, yield, and productivity were lower when 2,3-BDO was amassed by *E. ludwigii* on crude xylose (63.5 g/L, 0.36 g/g; 0.84 g/L. h) from sugarcane bagasse [27].

Metabolic engineering approaches for enhancing 2,3-BDO production. For bulk production of 2,3-BDO, high TYP metrics are a prerequisite. Pursuant to these goals, many metabolic engineering approaches have been developed for ameliorating 2,3-BDO production (Table 2). The perusal of the literature shows that perturbations, including pathway/metabolic engineering, have been employed, which can be divided into three categories; reinforcement of 2,3-BDO pathway with homologous/heterologous overexpression; elimination of by-products emerging from pyruvate node; cofactor engineering for maintaining redox balance [24,31,35].

2.2. 1,3-Butanediol (1,3-BDO)

1,3-BDO is a non-native metabolite and is not naturally synthesized by microorganisms. It exists in the form of two stereoisomers, R-1,3-BDO and S-1,3-BDO. The chemical manufacturing route results in a racemic mixture of R and S forms of 1,3-BDO. Optically active 1,3-BDO finds application as the building block for antibiotics, pheromones, fragrances, insecticides, and ß-lactam antibiotics, while the racemic mixture is used as an organic solvent in food and cosmetic industries [36]. 1,3-Butanediol (1,3-BDO) has a global market valuation of USD 344.61 million in 2022 and is expected to be USD 467.78 million by 2028 at a compound annual growth rate of 5.23% [37].

The enzymatic bioconversion of 4-Hydroxy-2-butanone (4H2B) to 1,3-BDO has been investigated and demonstrated in several microorganisms, *Kluyveromyces, Candida, Pichia,* and others, as well as engineered *Escherichia coli* [38,39]. As there are no natural organisms that can generate 1,3-BDO as an intermediate or end product, microorganisms have been engineered with the introduction of artificial pathways combining either enzymes β-ketothiolase, acetoacetyl-CoA reductase, and aldehyde/alcohol dehydrogenase or pyruvate decarboxylase. aldolase and aldehyde dehydrogenase. The overall pathway for 1,3-BDO production from glucose can be divided into two parts. The first, naturally occurring part includes the generation of central carbon intermediate (pyruvate and acetyl-CoA) and reducing equivalents [NAD(P)H], whereas the second part involves two alternative routes for converting pyruvate or acetyl-CoA into 1,3-BDO (Fig. 1). Two molecules of acetyl-CoA undergo self-condensation to give acetoacetyl-CoA, mediated through β-ketothiolase. In the next step, acetoacetyl-CoA is reduced to 3-hydroxybutyryl-CoA using electrons from NAD(P)H and catalysed by acetoacetyl-CoA reductase. The last two steps involve the reduction of 3-hydroxybutyryl-CoA to 1,3-BDO via 3-HBAD by aldehyde/alcohol dehydrogenase through electrons coming from NADH. Since the production route

requires excess reducing equivalents to reduce keto and aldehyde groups, the 1,3-BDO pathway is considered a reductive pathway. Table 3 compares the microbial 1,3-BDO production carried out by different research groups in the last decade.

Escherichia coli. *E. coli* is the most explored organism for developing as a cell factory for 1,3-BDO production. The native pathway of 1,3-BDO from biomass has not been identified and is a non-natural synthon. The first report on the biosynthesis of (*R*)-1,3-BDO from glucose by metabolically engineered *E. coli* was by Kataoka et al. [40]. To build synthetic pathway, the following genes were investigated:: *phaA* (encoding β-ketothiolase); *phaB*/*hbd* (encoding acetoacetyl-CoA reductase); *bld* (butyraldehyde dehydrogenase); *adhE* (aldehyde/alcohol dehydrogenase). The genes *phaA* & *phaB* were outsourced from *Ralstonia eutropha/C. necator*, while *adhE* & *hbd* and *bld* was taken from *Clostridium acetobutylicum* and *Clostridium saccharoperbutylacetonicum*, respectively. These four genes were employed in different combinations (**A:** *phaA+adhE+phaB*; **B:** *phaA+adhE+hbd*; **C:** *phaA+bld+phaB*; **D:** *phaA+bld+hbd*) to introduce the four synthetic pathway in *E. coli*. Among the four pathways tested, only A and C yielded 1,3-BDO at 0.37 and 1.45 mM, respectively. Since pathway C contained only butyraldehyde dehydrogenase, it was assumed that the last step of reduction of 3-hydroxybutyryl-CoA to 1,3-BDO was catalysed by the native enzyme of the host. The balance of gene selection and synchronization between gene products is necessary for high efficiency of the pathway as high overexpressed genes or too high enzyme activity may result in an imbalanced metabolism. For example, high activity of any of the last three enzymes will result in excessive consumption of NADH, draining out redox cofactor for other enzymes.

The recombinant strain with pathway C was further optimized in terms of IPTG concentration, oxygen supply, and pH. The smooth production of 1,3-BDO requires a continuous supply of acetyl-CoA and NAD(P)H, which is facilitated by aerobic conditions, while butyraldehyde dehydrogenase from *C. saccharoperbutylacetonicum* is an oxygen-sensitive enzyme. To mitigate the oxygen-sensitivity of butyraldehyde dehydrogenase from *C. saccharoperbutylacetonicum*, the oxygen level was optimized achieving an improved 1,3-BDO titer of 11.0 mM was achieved at a volume ratio of 1:7. Next, batch fermentation using resting cells was carried out. It was found that intermittent pH control (~6.0) improved glucose conversion and 1,3-BDO production and reduced piling up of acetate. The 1,3-BDO production achieved at 36 h was 34.6 mM (3.1 g/L). Finally, fed-batch cultivation with resting cells and pH control yielded 100.4 mM (9.0 g/L) 1,3-BDO at 110 h. In their next study, they optimized the oxygen transfer coefficient (82.3 h^{-1}) and pH (5.5). The batch and fed-batch fermentation using optimal value resulted in 98.5 (8.9 g/L) and 174.8 mM (15.7 g/L) 1,3-BDO with a yield of 0.44 and 0.37 mol/mol after 36 and 96 h, respectively [41].

In recent work, Liu et al. metabolically engineered *E. coli* for 1,3-BDO production from glucose, including screening key enzymes of the pathway, enhancing the supply of NADPH, elimination of by-products, and optimization of aeration [36]. Similar to Kataoka et al., they also outsourced *phaA* and *phaB* genes from *R. Eutropha* [40]. To catalyse the final step of the pathway, 3-HBAD to 1,3-BDO, endogenous *yqhD* was

overexpressed in *E. coli*, which is known to efficiently reduce a broad range of aldehydes. For catalysing the reduction of (R)-3-hydroxybutyryl-CoA, they screened four CoA-acylating aldehyde dehydrogenases with a broad substrate spectrum including an *ald* (butyraldehyde dehydrogenase), *bld*[L273T] (mutated butyraldehyde dehydrogenase), *pduP_St* (propionaldehyde dehydrogenases) and *pduP_Kp*(propionaldehyde dehydrogenases) genes from *Clostridium beijerinckii*, *Clostridium saccharoperbutylacetonicum*, *Salmonella typhimurium,* and *Klebsiella pneumoniae*, respectively.

The introduction of codon-optimized genes *yqhD, phaA, phaB,* and *bld*[L273T]via high-copy plasmid pTrc99a into an engineered *E. coli* W3110 strain (Δ*adhE*Δ*ldh*Δ*pta-ackA*) where metabolic pathways for ethanol, lactic and acetic acid were inactivated, resulted into 2.86 g/L (R)-1,3-BDO with optical purity >99%. This was the best result obtained among various Co-A acylating aldehyde dehydrogenase tested. They speculated that it could be due to the mutation in Bld at Leu273 within the active site that can stabilize the structure, leading to enhanced affinity towards NAD(P)H. The synthesis of one mole of 1,3-BDO requires three moles of NAD(P)H where two enzymes (acetoacetyl-CoA reductase/*phaB* and alcohol dehydrogenase/*yqhD*) of the pathway are highly specific to NADPH, indicating that a continuous NADPH supply is imperative for smooth 1,3-BDO production. To alleviate this bottleneck, *pntAB* genes encoding a membrane-bound proton-translocating transhydrogenase were overexpressed, which caused an increment in cell growth as well as 1,3-BDO production (4.12 g/L). The 1,3-BDO is significantly impacted by oxygen levels as Bld is an oxygen-sensitive enzyme, and high oxygen levels may reduce the availability of acetyl-CoA for 1,3-BDO synthesis by diverting it towards the TCA cycle. Further, they optimized aeration at flask levels by changing working volume and agitation speed, which helped in improving the 1,3-BDO level, but the strain also accumulated a substantial amount of 3-hydroxybutyric acid (3-HB). The maximum 1,3-BDO titer achieved under optimized conditions was 5.63 g/L with a yield of 0.56 mol/mol along with 2 g/L 3-HB and small amounts of ethanol, acetic and succinic acid. To divert accumulated 3-HB towards 1,3-BDO, 3-HB consuming pathway was combined with the 1,3-BDO pathway in two different plasmids. Carboxylic acid reductase (CAR) is known to catalyse the irreversible reduction of carboxylic acids and can reduce 3-HB to 3-HBAD, which can be further reduced to 1,3-BDO (Fig. 1). For this, carboxylic acid reductase (CAR) [from *Mycobacteroides abscessus* (CAR-B1)], *sfp* (encoding for phosphopantetheinyl transferase from *Bacillus subtilis* to activate the apoenzyme CAR), and *yqhD* genes were expressed on plasmid pCDFDuet-1 under the control of a Trc promoter, and the two resulting plasmids were transformed into *E. coli* strain. The fed-batch culture of the resulting strain amassed 13.4 g/L 1,3-BDO in 32 h with a conversion yield of 0.57 (mol/mol). The increase of 3HB pool in combination with the overexpression of *car* and inhibition of fatty acid synthesis enabled further improvement of titer (22.7 g/L) and yield (0.80 mol/mol) [42].

Nemr et al. also employed pyruvate-based pathways for 1,3-BDO synthesis in *E. coli* and combined metabolic and process engineering approaches for enhancing 1,3-BDO production [43]. The 3-HBAD can be reduced to 1,3-BDO by a variety of native aldehyde reductase present in *E. coli*, but these can also reduce acetaldehyde , available from decarboxylation of pyruvate, to ethanol. To avoid that, they searched for aldo-keto reductase

(AKR), specific towards 3-hydroxybutanal, which can avoid ethanol formation. They screened various enzymes and found the best combination of PDC, Dra/DERA (deoxyribose-5-phosphate aldolase), and AKR from *Zymomonas mobilis*, *Bacillus halodurans,* and *Pseudomonas aeruginosa*, respectively. The competing pyruvate draining pathways were deleted with the knock out of *adhE* (ethanol), *ldhA* (lactate), *pflB*(formate), and *poxB/pta* (acetate) genes. Due to higher PDC activity (carboligation) on acetaldehyde than Dra, it is converted to acetoin which, on subsequent reduction by promiscuous reductases, yields meso-2,3-BDO, another major by-product. To overcome this, two-stage fed-batch fermentation was conducted where the first growth stage was carried out aerobically, followed by microaerobic conditions for 1,3-BDO production to allow sufficient pyruvate flux and reducing power. The recombinant strain with *poxB/pta* deletions and two copies of Dra and AKR with strong RBS's accumulated 2.4 g/L of1,3-BDO with a conversion yield of 0.058 g/g of glucose.

In a most recent study, *E. coli* K12 MG1655 was chosen for enhanced 1,3-BDO production from glucose [44]. In the first stage, the two genes, namely *phaA*, *phaB* from *C. necator,* and one gene (*bld*) from *C. saccharoperbutylacetonicum* were introduced in the parent strain. Later, *yqhD* gene encoding from non-specific alcohol dehydrogenase from *E. coli* led to higher bioconversion of 3-HBAD to 1,3-BDO. Further genes encoding for lactate dehydrogenase (*ldhA*), alcohol dehydrogenase (*adhE*), pyruvate oxidase (*poxA*), phosphoacetyl transferase and acetate kinase (*pta-ackA*), and acyl-CoA thioesterase (*yciA*) were sequentially deleted, to reduce the by-product formation. The engineered strain and intensification of the bioprocess module led to a molar yield and productivity of 0.51 and 0.64 g/L/h, respectively, and a highest-ever reported titre of 23.1 g/L 1,3-BDO using the fermentative route [44]. Genomatica is currently the only commercial producer of bio-based 1,3-BDO , sold under the brand name Brontide™ and Alvea™ [45]. This diol is produced fermentatively by recombinant *E. coli* using renewable sugars as the feedstock [46]. However, the TYP matrices attained industrially are not disclosed in the public domain.

Cupriavidus necator. *C. necator* is well known native host for intracellular accumulation of biodegradable polymer poly-3-hydroxybutyrate (PHB). The metabolic pathway for PHB shares steps with the engineered route for 1,3-BDO production. Based on the high availability of 3-hydroxybutyryl-CoA (3-HB-CoA) and pyruvate precursors in *C. necator*, Gascoyne et al. employed two different routes referred as 3-HB-CoA and pyruvate pathways, respectively, for the biosynthesis of 1,3-BDO [47]. The first one was the same as described starting with the condensation of acetyl-CoA to acetoacetyl-CoA followed by two reduction steps to 1,3-BDO via 3-HB-CoA and 3-HBAD. Being a native producer of PHB, *C. necator* already has the first two steps of the pathway. The carbon flux towards 1,3-BDO was enhanced by blocking PHB formation and deletion of genes of the TCA cycle. The designed pathway consisted of acetyl-CoA acetyltransferase (*phaA*), acetoacetyl-CoA reductase (*phaB*), 3-hydroxybutyryl-CoA dehydrogenase (*bld),* and NAD(P)H-dependent alcohol dehydrogenase (*yqhD*). The *phaA* and *phaB* are endogenous to *C. necator* H16 and provide a precursor to 3-HB-CoA, while *bld* and *yqhD* were outsourced from *Clostridium saccharoperbutylacetonicum* and *E. coli*, respectively, for converting 3-hydroxybutyryl-CoA to 1,3-BDO. To divert 3-HB-CoA towards (*R)*-1,3-BDO, the *phaC1* gene encoding for poly(3-

hydroxyalkanoate) polymerase for PHB synthesis was knocked out from the chromosome. They also attempted deletion of genes (*sucCD*, *iclAB*) of the TCA cycle to maximize acetyl-CoA pool towards biosynthesis of 1,3-BDO and showed that elimination of *sucCD* improved 1,3-BDO yield. The second pathway involved decarboxylation of pyruvate to acetaldehyde by pyruvate decarboxylase (PDC) followed by aldol condensation of acetaldehyde by deoxyribose-5-phosphate aldolase (Dra/DERA) to give 3-HBAD. The final step includes the reduction of 3-HBAD to 1,3-BDO by NADPH-dependent aldehyde reductase. This pathway requires only one NADPH, whereas 3-HBCoA consumed 3 NADPH. However, the pathway was unable to generate a detectable amount of 1,3-BDO. Notably, there was no accumulation of pyruvate, and high yields of acetate and ethanol were observed, indicating the inability of Dar to transform acetaldehyde into 3-HB-CoA.

Subsequently, the combination of both pathways, pyruvate, and 3-HB-CoA pathways, and to this end, *bld*, *yqhD*, *dra,* and *PDC* were assembled into a plasmid. The recombinant strain containing two pathways showed 1.7-fold improvement in 1,3-BDO production compared to the control strain containing only 3-HB-CoA pathway. Further, to allow controllable expression, all these four genes were integrated into *phaC* locus, which also abolished PHB synthesis. To increase the copy number, an engineered strain containing chromosomally integrated pathways was transformed with a plasmid carrying *bld* and *dra* copies. The extra copy of *bld* caused significant enhancement in 1,3-BDO yield; however, *dra* had an insignificant impact. *C. necator* is a facultative lithoautotrophic bacterium and can grow using CO_2 as a carbon source. The autotrophic fed-batch cultivation of recombinant *C. necator* strain {H16Δ1::56-p14 H16Δ*phaC1*::*P[bldyqhD_{Ec}dra PDC phaAB]* (*P[bld]*)} generated 2.97 g/L (33 mM) 1,3-BDO in 120 h with a yield of 0.40 c_{mol}/c_{mol}. The accumulation of a substantial amount of 4-hydroxy-2-butanone (19.7 mM), the oxidized form of 1,3-BDO, reflects the insufficient conversion of acetoacetyl-CoA to 3-HBADby PhaB.

Cell-free synthesis. In a very interesting work, Liu and Bowie developed a carbon-negative emission technology for converting ethanol carbon into 1,3-butanediol via cell-free synthesis [48]. The pathway starts with the oxidation of ethanol, a non-spontaneous reaction, which was made feasible by coupling with NADH oxidase (NOX). NOX oxidizes NADH to NAD+ (NADH + O_2 → NAD+ + H_2O; -442.8 KJ/mol) to drive ethanol oxidation to acetaldehyde (Ethanol + NAD+ → Acetaldehyde + NADH; +21.7 KJ/mol) by alcohol dehydrogenase (ADH). In the next step, acetaldehyde undergoes aldol condensation to give 3-HBADby a promiscuous aldolase 2-deoxy-d-ribose-5-phosphate aldolase (DERA). Finally, 3-HBAD is reduced to 1,3-BDO, a specific aldo-ketol reductase (AKR). The reducing power (NADPH) for this reaction was provided through the oxidation of formate by the enzyme formate dehydrogenase (FDH) (Formate + NADP+ → CO_2 + NADPH). The released CO_2 can be transformed back into formate electrochemically. Though ADH and AKR are specific for their cofactors, ADH can use NADP+ and produce NADPH which could be utilized by AKR and vice versa. Thus, a measurable crossover between two enzymes could allow 1,3-BDO production in the absence of formate. With an initial ethanol concentration of 140 mM, the batch reaction produced 60 mM 1,3-BDO by day 3, corresponding to 85% conversion. Since ethanol was completely consumed, the remaining 15% mass accumulated in intermediates

or unidentified side products. To further boost the 1,3-BDO production, the initial ethanol concentration was increased to 350 mM, and further, 88 mM ethanol and 30 mM formate were added after every day of reaction. Due to the inhibition of NOX and DERA enzymes in the presence of alcohols, the reaction medium was supplemented with these enzymes in proportion to the expected loss of activity. About 45 mM of 1,3-BDO was accumulated after day 1 and was slowed down on day 2 and 3. Even in the absence of ethanol consumption, 1,3-BDO formation continued indicating slow conversion of intermediates into the product. The final 1,3-BDO titer generated after 4 days was 85 mM (7.7 g/L) with a productivity of 0.16 g/L. h.

2.3. 1,4-Butanediol (1,4-BDO)

1,4-BDO is another industrially important large-volume commodity chemical with applications in the food, chemical, medical, and pharmaceutical industries. 1,4-BDO is used as starting material for manufacturing polybutylene terephthalate, tetrahydrofuran (THF), γ-butyrolactone (GBL), polybutylenesuccinate, etc. [49]. Almost 50% of 1,4-BDO produced globally is consumed in THF production, and around 35% is used in the polymer industry to produce polybutylene terephthalate, polyurethanes, and biodegradable polybutylene succinate, with the balance being used in the production of GBL [50]. It has applications ranging from automotive plastics and electronics to sneakers, soccer balls, and spandex for apparel [51]. As per Verified Market Research, the global 1,4-BDO market in 2018 was $7.8 billion and is forecasted to reach $14.5 billion by 2026 [52,53]. As a result, there have been a couple of articles on the biosynthesis of 1,4-BDO using cell factories in the last two decades (Table 4).

Glucose-based biosynthesis of 1,4-BDO. Metabolic Engineering is a very powerful tool for designing high-performing cell factories to transform cheap renewable feedstocks into chemical building blocks. 1,4-BDO is not part of microbial metabolism, and no known organism produces it as an intermediate or end product. Further, 1,4-BDO is a highly reduced molecule and requires a strong reducing power and a huge energy supply for continuous and smooth production, which poses another challenge. The biochemical pathway for 1,4-BDO production does not generate any ATP, so the energy required for growth, maintenance, transport, and other cellular activities must come from respiration [51]. The metabolic route to 4-hydroxybutyrate (4-HB) (Fig. 2) starts from succinate, which is activated to succinyl-CoA by succinyl-CoA synthetase (SucCD), followed by the reduction in two consecutive steps to 4-HB via succinyl semialdehyde by CoA-dependent succinate semialdehyde dehydrogenase (SucD) and 4-HB dehydrogenase (4-HBd). The CoA derivatization of 4-HB using acetyl-CoA yields 4-HB-CoA, which on reduction to 4-hydroxybutyraldehye and then 1,4-BDO in the next two steps by enzymes 4-hydroxybutyryl-CoA transferase, 4-hydroxybutyryl-CoA reductase, and alcohol dehydrogenase, respectively. The pathway can also start with α-ketoglutarate, another intermediate of the TCA cycle. The decarboxylation of α-ketoglutarate gives succinyl semialdehyde catalysed by 2-oxoglutarate decarboxylase (SucA). Owing to irreversible decarboxylation, this route is thermodynamically favourable and consumes less reducing power than succinate route [18,51]. In 2011, Yim et al. metabolically engineered *E. coli* to introduce a synthetic pathway for 1,4-BDO from glucose using a combination of native and heterologous

enzymes [18]. In cell metabolism, the TCA cycle is the major source of reducing equivalents, and to divert them toward metabolite production, their oxidation by the electron transport chain should be avoided. The real challenge is to run the TCA cycle in oxidative mode and make it fully functional under anaerobic or oxygen-limited conditions. Therefore, the strain was designed for anaerobic operation of the TCA cycle to maximize the generation of reducing power to drive 1,4-BDO production. The pathway was divided into two parts, from glucose to 4-hydroxybutyrate (4-HB) and 4-HB to 1,4-BDO. After successful establishment, these two parts were connected to construct a single route. For establishing glucose to 4-HB route, the synthetic operon consisting of *sucCD* (from *E. coli*), *sucD,* and *4hbd* (from *Porphyromonas gingivalis*) were introduced into the host strain, and maximum 4-HB production (11 mM) was achieved with the strain containing medium copy plasmid. For 4-HB to 1,4-BDO production, overexpression of 4-hydroxybutyryl-CoA transferase (*cat2*) gene from *P. gingivalis* on the medium-copy plasmid and *adhE2* gene from *Clostridium acetobutylicum* on the high-copy plasmid pZE13S led to 138 µM 1,4-BDO in the culture broth. They also optimized the arrangements and copy number of plasmids along with codon optimization to maximize the expression. Finally, both the segments were assembled together on two plasmids pZA33S-*sucCD-sucD-adhE2* and pZE13S-*cat2-4hbd*, the recombinant strain resulted in 0.6 mM BDO along with 2.1 mM 4HB and 6.2 mM succinate from 20 g/L glucose in 48 h.

To maximize 1,4-BDO yield further, alcohol dehydrogenase (*adhE*), pyruvate formate lyase (*pflB*), and lactate dehydrogenase (*ldhA*) genes were knocked off to block ethanol, formate, and lactate formation. The strain with deletion of these genes, specifically *pflB*, exhibited poor growth due to NADH sensitivity of the E3 subunit (encoded by *lpdA*) of the pyruvate dehydrogenase complex. To overcome this, the native *lpdA* gene was replaced with the *lpdA* gene of *Klebsiella pneumoniae* with D354K mutation, known to reduce NADH sensitivity. Though the resulting strain did not grow under strictly anaerobic conditions, it performed much better when cultured in a microaerobic environment. The fed-batch culture of this strain (*ΔadhEΔpflBΔldhAΔlpdA:: Kp.lpdD354K*) with plasmids containing the entire BDO pathway accumulated 82 mM 1,4-BDO in 48 h. Acetate, pyruvate, and ethanol were obtained as major by-products, even more than 1,4-BDO, while 4-HB was obtained in comparable amounts with a small amount of GBL, lactonized form of 4-HB. 1,4-BDO pathway requires a large amount of reducing power, and therefore, to achieve this, it is important to operate the TCA cycle in oxidative mode rather than reductive one, generating eight reducing equivalents from one mole of glucose. The *mdh* gene encoding malate dehydrogenase, a key enzyme of the reductive TCA cycle, was eliminated to allow more carbon flux through the oxidative TCA cycle. Further, *arcA* gene, a transcriptional repressor of several genes expressed under aerobic conditions, was deleted for enhanced expression of citrate synthase, aconitase, and isocitrate dehydrogenase, and a mutation (R163L) was introduced in gene *gltA* (citrate synthase) to make it less sensitive to NADH inhibition. When the resulting strain (*ΔadhEΔpflBΔldhAΔmdhΔarcAΔlpdA:: Kp.lpdD354K gltAR163L*) with all these modifications was transformed with plasmid containing complete 1,4-BDO pathway, including α-ketoglutarate decarboxylase (*sucA*), the amount of 1,4-BDO amassed was more than 4-HB and succinate accumulation was abolished due to removal of reductive TCA pathway. They found that the aldehyde

dehydrogenase gene (025B) from *Clostridium beijerinckii* encoding a monofunctional enzyme, with aldehyde dehydrogenase activity only, was not only very active in the conversion of 4-HB-CoA to 1,4-BDO but also produced much less ethanol in comparison to bifunctional aldehyde and alcohol dehydrogenase enzyme (002) from *Clostridium acetobutylicum*. The fed-batch cultivation of recombinant strain (*ΔadhEΔpflBΔldhAΔmdhΔarcAΔlpdA:: Kp.lpdD354K gltAR163L*pZS*13S-*sucCD-sucD-4hbd*/*sucA*pZE23S-*adh*(025B)-*Cat2*) yielded 18 g/L 1,4-BDO in five days with yield of 0.37 g/g. Pyruvate, acetate, and ethanol production was substantially reduced, while the 4-HB level was enhanced.

Although the rewiring of *E. coli* by Yim et al. was successful in rerouting the carbon flux towards a non-native 1,4-BDO, there were still lots of bottlenecks to be overcome, and this work was continued by Genomatica to production levels [18]. The main challenge was to weaken the by-product formation and avoid carbon loss in the form of acetate (*ack-pta*), formate (*pflB*), lactate (*ldhA*), pyruvate, GBL (*YbgC*), gamma-aminobutyric acid (GABA) (*PuuE*) and CO_2. The knockout of these by-products would be able to promote carbon flux towards 1,4-BDO [49,51,54]. To reduce the by-product, *sad* and *gabD*, encoding for succinate semialdehyde dehydrogenases and converting succinyl-semialdehyde back to succinate were deleted, and this led to a significant increment in 1,4-BDO titer to 29 g/L [54]. Similarly, Burgard et al. knocked out *PuuE* (aminotransferase) and observed a noticeable drop in GABA formation [51], and Wu et al. eliminated *Sad* (succinate semialdehyde dehydrogenase) and *Ybgc* (acyl-CoA thioesterase), which decreased levels of GBL and succinate by 55% and 83% respectively [55]. Several approaches were employed to debottleneck: reduced pathway enzymes activity or expression, energy limitations and redox imbalance in host metabolism, unfavourable thermodynamics, fermentation, end product toxicity, and downstream processes. For example, the discovery of new enzymes coupled with directed evolution efforts for downstream pathway enzymes Cat2, Ald, and Adh improved enzyme activity, rate, and selectivity. Further, the combination of best-performing enzymes under constitutive promoters eliminated the requirement for inducers and antibiotics [54]. All these changes resulted in a remarkable increase in titer (99.0 g/L), yield (0.35 g/g), and productivity (2.1 g/L. h).

They carried out diagnostic experiments and found that 1,4-BDO toxicity and impaired driving were not constraining production during the later stage of fermentation, and energy and redox balance were not restricting biosynthesis. Rather, the focus should be on downstream pathway enzymes mediating the conversion of 4-HB to 1,4-BDO, i.e., Cat2 and Ald. GBL is a by-product during 1,4-BDO synthesis, upstream of Ald and downstream of Cat2, which accumulates in strains devoid of GBL lactonase. The accumulation and profile of GBL, along with diagnostic experiments, revealed that Cat2 and/or Ald were responsible for the drop in BDO productivity during the later stage. To overcome this, a directed enzyme evolution approach was used, and libraries of mutant strains of Cat2 and Ald were created and screened. The promising variants with enhanced activity, expression, and stability were identified. The use of strain containing evolved variants of Cat2 and Ald caused 75% reduction in 4-HB and 20% increment in 1,4-BDO titer to 110 g/L. Finally, by-product (acetate, ethanol, glutamate, 4-aminobutyrate, and CO_2) formation was reduced to a large extent to improve product yield and reduce product

separation cost. We will describe a few of them. In 1,4-BDO accumulating strain, the fast operation of oxidative TCA cycle maintains low acetyl-CoA levels through a strong irreversible pull to push *ackA* (acetate kinase)-*pta* (phosphotransacetylase) equilibrium in reverse direction towards acetyl-CoA production from acetate. Therefore, acetate accumulation was attenuated via overexpression of *ackA-pta* with a constitutive promoter. Ethanol production was cut down through overexpression of phosphoenolpyruvate carboxylase (*ppc*), diverting pyruvate towards oxaloacetate, which is utilized for the oxidative TCA cycle along with acetyl-CoA, precursor for ethanol. GABA is produced from succinate semialdehyde, a BDO pathway intermediate and its formation was blocked by eliminating the *gabT* and *PuuE* genes encoding aminotransferase enzymes [56,57]. The ^{13}C-flux analysis indicated that CO_2 was mainly coming from the oxidative pentose phosphate pathway (PPP) and TCA cycle, indicating a clear competition between PPP/TCA cycle and 1,4-BDO pathway. This is in excess of CO_2 coming from production of 1,4-BDO from sugars ($C_6H_{12}O_6 + 0.5O_2 \rightarrow C_4H_{10}O_2 + 2CO_2 + H_2O$). To curb CO_2 levels, *zwf* and *sdhABCD* were deleted, which resulted in growth defects and diminished 1,4-BDO production. These defects were restored by the deletion in the electron transport chain and optimized *pntAB* (membrane-bound transhydrogenase) overexpression and formate supplementation to provide ATP via oxidative phosphorylation, leading to 50% reduction in CO_2. Finally, all these modifications were introduced in one strain, and the optimized fermentation with the fed-batch culture of engineered *E. coli* generated 1,4-BDO titer >125 g/L with yield >0.40 g/g and productivity >3.5 g/L.h [58]. The commercial strain for bio-based production of 1,4-BDO production from glucose can accumulate ~140 g/L. This is the highest titer of 1,4-BDO achieved so far. In comparison to the chemical route, the industrial bioprocess is proven to reduce CO_2 emissions/kg of BDO and fossil energy usage by 83% and 67%, respectively. Presently, Genomatica is the only company that is commercially producing bio-based 1,4-BDO under the trade name GENO BDO™ [59].

1,4-BDO production from xylose and other sugars. 1,4-BDO production has also been attempted from pentose sugars, including xylose, and the metabolic pathway has multiple advantages compared to the glucose-based pathway. Fig. 3 describes three biochemical routes for 1,4-BDO synthesis from xylose [49,60,61]. The xylose-based pathway bypasses the TCA cycle, avoids the acetyl-CoA node, and has shorter steps with less requirement of reducing equivalents. However, the pathway cannot generate 1,4-BDO from glucose or sucrose. There are three routes for the conversion of xylose into 1,4-BDO. In the first pathway, xylose is dehydrogenated to xylonic acid by xylose dehydrogenase (*xdh*) followed by two consecutive two dehydration steps to generate α-ketoglutaric semialdehyde by D-xylonic acid dehydratases (*yjhG* and *yagF*) and 2-dehydro-3-deoxy-D-xylonate dehydratase (*xylX* and *hvo*), respectively. The α-ketoglutaric semialdehyde is reduced to 5-hydroxy-α-ketoglutarate by alcohol dehydrogenase (*sadh*). which upon decarboxylation by keto-acid decarboxylase (*mdlC* and *kivD*) yields 4-hydroxybutyraldehyde, and reduction of it by alcohol dehydrogenase (*adh*) results in 1,4-BDO. Liu and Lu made use of this pathway into *E. coli*, and the metabolic engineering and synthetic biology work was partitioned into two functional parts: enzymatic reactor and genetic controller [60]. Similarly, the division of carbon source utilization was made into two independent routes so that glucose was used for cellular

growth while xylose was exclusively channelized for 1,4-BDO formation. This approach will minimize the crosstalk between the two parts and expedite the pathway engineering and optimization. To prevent carbon flux towards PPP and Dahms pathway, the xylose isomerase gene (*xylA*) and 2-dehydro-3-deoxy-D-xylonate aldolase genes (*yjhH* and *yagE*) were knocked off from the genome to disable the ability of the strain to grow on xylose or xylonic acid and do not interfere with cellular growth on glucose to decouple biomass and product formation. The enzymes were outsourced from various organisms, and the optimal combination of the enzyme was assembled to maximize 1,4-BDO production. The aerobic cultivation of engineered *E. coli* accumulated 0.44 g/L 1,4-BDO with a conversion yield of 0.042 g/g from xylose. The second pathway involves non-phosphorylative uptake of sugars into the TCA cycle in less than six steps, making it more energy efficient than the conventional route. The pathway starts with converting xylose to xylonolactone by xylose dehydrogenase (*xylB*), followed by hydrolysis of it to xylonate by the action of xylonolactonase (*xylC*). The two consecutive steps of dehydration of xylonate generate 2,5-dioxopentanonate (DOP) via 2-keto-3-deoxy-D-xylonate by xylate dehydratase (*xylD*) and 2-keto-3-deoxy-D-xylate dehydratase (*xylX*), respectively [62]. The decarboxylation of DOP mediated by 2-keto acid decarboxylase (*KDC*) yields 1,4-butanedial, which is transformed to 1,4-BDO, catalyzed by alcohol dehydrogenase (*adh*). The total number of steps in the pathway, from pentose sugars to 1,4-BDO, is six (Fig. 3). Tai et al. created this synthetic pathway into *E. coli* for production of 1,4-BDO from D-xylose, L-arabinose, and D-galactouronic acid [62]. For xylose-based production, xylose operon (*xylBCDX*) was cloned from *Caulobacter crescentus,* and the endogenous xylose (*xylA*) and xylonate (*yagE* and *yjhH*)-consuming pathways were eliminated. They removed isocitrate dehydrogenase (*icd*) so that the cell requires a supply of α-ketoglutarate and this could be fulfilled through the reduction of DOP by α-ketoglutarate semialdehyde dehydrogenase (KGSADH), a key intermediate of the TCA cycle and PPP. To make the pathway more efficient, they screened and engineered downstream pathway enzymes to identify the best 2-ketoacid decarboxylases and alcohol dehydrogenases. They found that KDC (KivD) from *Lactococcus lactis* was identified as the best KDC toward DOP, and the best combination was Kivd with YqhD (from *E. coli*) yielding 0.15 g 1,4-BDO/g xylose. However, the yield of by-product 1,2,4-butanedtriol (0.28 g/g) was almost two-fold higher than the main product. This is due to the promiscuous nature of KivD and less selectivity for decarboxylation of DOP and can also decarboxylate 2-keto-3-deoxy-D-xylonate into 1,2,4-butanedtriol, leading a higher titer. To overcome this, protein engineering of KivD was carried out to shrink the binding site to make better fit and selectivity for DOP than bulkier 2-keto-3-deoxy-D-xylonate, and KivdV461I was found as the best variant. The fermentation using KivdV461I produced 3.83 g/L BDO with only 0.99 g/L BTO. The xylose + glucose co-fermentation of final recombinant *E. coli* strain [*ΔxylAΔyagEΔyjhH ::xylB-xylC-xylD-xylXkivd(V461I)-yqhD*] in a fed-batch mode accumulated 9.2 g/L 1,4-BDO in 36 h from consumption of 42.1 g/L of xylose while glucose was fed to support cell growth. To enable the co-production of 1,4-BDO and mevalonate (MEV), the MEV pathway was introduced, and the engineered strain accumulated 12.0 g/L 1,4-BDO from the assimilation of 46 g/L xylose along with ~20 g/L of MEV in 30 h. This strategy enhanced the yield of 1,4-BDO from 36% to 43% of

the theoretical maximum. The accumulation of acetate (11 g/L) inhibited the production of both metabolites. *E. coli* was also engineered extensively for 1,4-BDO production from arabinose and galactouronic acid. The engineered strain generated 15.6 and 16.5 g/L 1,4-BDO in 72 and 90 h from 70.5 and 50.5 g/L of arabinose and galacturonic acid with a yield of 37% and 70% of the theoretical maximum.

The third route makes use of the diol dehydratase enzyme and involves 1,2,4-butanedtriol as one of the intermediates. Xylose is oxidized to xylonic acid by xylose dehydrogenase, which is acted upon by xylose dehydratase to 3-deoxy-glycerol pentulosonic acid whose decarboxylation by α-ketoglutarate decarboxylase yields 3,4-dihydroxybutanal. The reduction of 3,4-dihydroxybutanal by alcohol dehydrogenase gives 1,2,4-butanedtriol, which is transformed into 4-hydroxybutyraldehyde by the action of diol dehydratase. In the final step, 4-hydroxybutyraldehyde is reduced to 1,4-BDO by alcohol dehydrogenase. Wang et al. exploited this route to synthesize 1,4-BDO from xylose [61]. The main challenge was to design a diol dehydratase to act on 1,2,4-butanedtriol, a rate-limiting step of the pathway. The diol dehydratase from *Klebsiella oxytoca* was engineered using rational approaches to improve the activity towards non-native substrate 1,2,4-butanedtriol. Diol dehydratase is well known to dehydrate 1,2-propanediol to propanal and the catalytic activity of the engineered enzyme towards 1,2,4-butanedtriol was enhanced by five-fold. For biosynthesis of 1,4-BDO from xylose, xylose dehydrogenase (*xylBC*) and xylonic acid/xylonate dehydratase(*xylD*) were outsourced from *C. crescentus* and α-ketoisovalerate decarboxylase (*kivD*) was borrowed from *L. lactis* while alcohol hydrogenase (*yqhD*) was native to *E. coli*. The competing pathways for xylose consumption were disrupted; xylose isomerase (*xylA*) and aldolase (*yagE* and *yjhH*). All these modifications resulted in 1,2,4-butanedtriol production of 1506 mg/L and to transform 1,2,4-butanedtriol into 1,4-BDO, variant S301AQ336AV300M of mutant diol dehydratase (*ppdA-C-B*) was overexpressed, which resulted in 1,4-BDO production of 209 mg/L and ~1209 mg/L of 1,2,4-butanedtriol was left unconsumed.

Besides the above-mentioned substrates, it has been proved that erythritol can also be a starting material for 1,4-BDO production. Erythritol, a C_4 polyol, is manufactured at an industrial scale from traditional carbon sources such as glucose, glycerol, or sucrose. The advantageous features of erythritol-based production of 1,4-BDO are structural similarity between erythritol and 1,4-BDO; shorter pathway with four steps only; the pathway requires only two enzymes with one being endogenous, reducing the metabolic burden on the cell; alcohol dehydrogenase and diol dehydratase. Dai and associates introduced the synthetic pathway in *E. coli,* where erythritol is transformed into 3,4-dihydroxy-butyraldehyde (3,4-DHBA) by a mutant form of glycerol (GDHt) or diol dehydratase (DDHt) [63]. In the next step, 3,4-DHBA is reduced to BTO via alcohol dehydrogenase, followed by dehydration to 4-hydroxybutyraldehyde by a mutant of dehydratase. Finally, the reduction of 4-hydroxybutyraldehyde yields 1,4-BDO by alcohol dehydrogenase [63]. The mutant form of GDHt or DDHt was created using side-directed mutagenesis. *E. coli* strain overexpressing S302AQ337A mutant of GDHt and S301AQ336A mutant of DDHt where alcohol dehydrogenase is endogenous, accumulated 16.1 and 11.9 mg/L of 1,4-BDO with a molar yield of 0.012 and 0.008, respectively, after 20 h. In their study, the impact of various

process parameters, including substrate levels, cell density, pH, and temperature on 1,4-BDO production, was investigated, and 58.5 mg/L was achieved using optimal parameters [63].

Non-model microorganisms can also be exploited for C4 diol production. For example, recently identified *Pichia kudriavzevii* has evolved a high catalytic activity and stereoselectivity for the bioconversion of 4-hydroxy-2-butanone to (R)-1,3-butanediol enabling to obtain the titer of 85.60 g/L [64]. *Methylomicrobium alcaliphilum* has been engineered for 2,3-BDO production from methane [65]. To further improve efficiency, genetic manipulation protocols and tools for non-model organisms need to be developed to address existing challenges associated with their application for BDO production.

3. Chemo-catalytic conversion of butanediols

BDOs are highly functional molecules and have vast derivatization chemistry with diverse product opportunities. The dehydration reaction using solid-acid catalysts is the dominant mechanism for producing high-value chemicals from BDOs. BD is the most vital BDO dehydration product and is the widely used building block in manufacturing synthetic rubber, elastomers, and resins [66]. At present, greater than 95% of BD is manufactured by steam cracking of naphtha [67]. Therefore, sustainable BD production from bioethanol [66] and bio-BDOs [13] has been gaining tremendous attention in recent times. BD can be obtained from all three BDO isomers via the 1,2-elimination reaction. The BDO dehydration reaction proceeds through unsaturated alcohols (UOL) intermediates, such as 3-buten-2-ol (3B2OL), 3-buten-1-ol (3B1OL), and 2-buten-1-ol (2B1OL). Methyl ethyl ketone (MEK) is another prominent BDO dehydration product with versatile applications as an industrial solvent [68,69]. Currently, MEK is manufactured by 2-butanol dehydrogenation using Cu or Zn catalysts. Renewable MEK can be obtained by pinacol rearrangement reaction of 2,3-BDO. However, MEK cannot be derived from 1,4-BDO due to the lack of a secondary hydroxyl group. Tetrahydrofuran (THF) is another important chemical obtained by cyclodehydration of 1,4-BDO. Dehydrogenation is another prominent reaction pathway for transforming BDOs into valuable derivatives. This route provides acetoin, diacetyl, and butylenes from 2,3-BDO, GBL from 1,4-BDO, and 4-hydroxy-2-butanone (4H2B) from 1,3-BDO. This section presents a comprehensive overview of chemo-catalytic upgrading of 2,3, 1,4, and 1,3-BDO into valuable chemicals.

3.1. 2,3-Butanediol

Methyl ethyl ketone (MEK). MEK and isobutyraldehyde (IBA) are formed from 2,3-BDO by pinacol rearrangement reaction with hydride and methyl shift over solid-acid catalysts (Fig. 4). Generally, MEK dominates over IBA as hydride shift is much faster than methyl shift [70]. However, high temperatures enhance methyl shift with increased IBA formation [71]. Besides, MEK selectivity is affected by two other competing dehydration reactions: (i) single and (ii) double dehydration via 1,2-elimination to 3-buten-2-ol (3B2OL) and BD, respectively. MEK is a thermodynamically favoured product at relatively low temperatures (180-300 °C) and high weight hourly space velocity (WHSV) [72,73]. However, slightly higher reaction temperature and smaller WHSV turn reaction selective towards 3B2OL, with BD as a minor product. Further rise in reaction temperatures improves selectivity to BD and IBA.

γ-Al_2O_3 and phosphates, such as aluminium phosphate and zirconium phosphate, have acidic properties and showed reasonable MEK selectivity at moderate temperatures (Table 5) [73,74]. However, elevated temperatures deteriorated MEK selectivity, simultaneously enhancing BD [74]. The catalytic activity of Al_2O_3 was also compared with H-BEA and Zr-BEA zeolites [73]. Al_2O_3 showed higher MEK selectivity than H-BEA and Zr-BEA due to its lower acidity, while Zr-BEA was selective toward C_8-C_{12} hydrocarbons formed by condensation of olefins [73]. The strong acidic site of H-BEA was reported to favour methyl shift [75]. To suppress IBA formation by methyl shift, strong acid sites of HZSM-5(360) were neutralized by phosphate modification, with concurrent enhancement of weak and medium acid sites [75]. 2% P/HZSM-5 thus showed excellent 2,3-BDO conversion and high MEK selectivity at low temperatures [75]. Further, ZSM-5 was modified with boric acid to improve catalytic stability and 2,3-BDO activation at low temperatures. Boric acid generates extra-framework B-OH species with better protonation ability, retaining silanol functional groups and improving effective acidity [71]. 1 wt% Boric acid loaded HZSM-5 thus showed better performance than HZM-5, with 97% 2,3-BDO conversion and 68% MEK selectivity at 180 °C [71]. Similar studies were also reported using amorphous calcium phosphate [76] and SiO_2-supported sodium phosphate [77].

3-Buten-2-ol (3B2OL). 3B2OL is a valuable chemical used to produce various organics, agrochemicals, and pharmaceuticals. It is formed as an intermediate during vapor-phase dehydration of 2,3-BDO [77–80]. The reaction requires bifunctional catalysts to anchor the -OH group on acidic sites and β-H on basic sites to obtain high 3B1OL selectivity (Fig. 5). Monoclinic ZrO_2 having redox properties thus showed good catalytic performance (Table 6) [78]. However, 3B2OL selectivity was poor due to the weak basicity of ZrO_2 [79]. ZrO_2 was thus modified by alkaline earth metal oxides (CaO, SrO, BaO, and MgO) to enhance basic site density [79,80]. The modifications resulted in highly dispersed metal-O-Zr hetero-linkages generating new acidic and basic sites with proper acid-base balance and higher 3B2OL selectivity [80]. However, modified ZrO_2 exhibited weaker acidity with lower 2,3-BDO conversion than pure ZrO_2. Among different alkaline earth metal oxides, BaO/ZrO_2 showed the maximum 2,3-BDO conversion [80]. The silica-supported alkali (Na, K, and Cs) phosphates have conjugated acid-base pairs formed by end groups of polyphosphates having P-OH and P-O⁻M⁺ entities in proximity [70,77]. These alkali phosphates with low Metal/P ratio thus showed high 3B2OL selectivity with reasonable 2,3-BDO conversion at elevated temperatures. However, K_P/SiO_2 and Cs_P/SiO_2 have a greater density of conjugated acid-base pairs than Na_P/SiO_2 and thus exhibited superior 3B2OL selectivity [70]. Rare earth oxides (REO), such as Sc_2O_3, have also shown promising catalytic activity with moderate 3B2OL selectivity [67].

1,3-Butadiene (BD). BD is formed by the two-step dehydration of 2,3-BDO and is prominent only at higher reaction temperatures (Table 7). The performance of REO in dehydrating diols is closely related to their ionic radii [81,82]. Sc_2O_3 having the smallest ionic radii exhibited excellent BD selectivity [67]. However, Sc_2O_3 is expensive. γ-Al_2O_3 is a cheaper alternative and exhibited good BD selectivity at relatively lower temperatures [83,84]. In another study, rare-earth orthophosphates demonstrated complete 2,3-BDO conversion with around 58% BD selectivity and good catalyst stability at 300 °C [85]. The dehydration reaction was reported to proceed

over Lewis acid-base sites to form 3B2OL, which was further dehydrated to BD over weak Brønsted acid sites. Weak Brønsted acidity of rare-earth orthophosphates, which was inadequate for pinacol rearrangement, was responsible for their exceptional BD selectivity [85]. Furthermore, the presence of water was found to improve catalyst stability by suppressing coke formation [85]. Silica-supported alkali phosphates, such as cesium and potassium-based phosphate, having a high density of acid-base conjugated pairs, exhibited good BD selectivity [70]. Similarly, silica-supported cesium dihydrogen phosphate (CsH_2PO_4) showed nearly 100% 2,3-BDO conversion with 91.9% BD selectivity at 400°C [86]. The exceptional catalytic performance of CsH_2PO_4 is attributed to its strong basic O_{neg} atom and the large ionic radii of Cs that suppresses interaction with the internal H atom of 2,3-BDO, promoting 1,2-elimination [86].

Acetoin and diacetyl. Acetoin has various applications as a food additive and cosmetic product, while diacetyl is used in food and beverage for flavour [87]. They are produced by 2,3-BDO dehydrogenation using copper-based catalysts (Table 8). The synergetic effect between Cu^o and CuO-like phase (-Si-O-Cu-O-Si-) plays a role in this reaction [87]. The Cu^{2+}-O^{2-} pair promotes the O-H bond cleavage, while the H atom from α-C is extracted by Cu^0 sites [87]. However, the dialkoxy group strongly adsorbs on Cu^0 sites, deactivating Cu/SiO_2 catalyst [87]. Nonetheless, Cu/SiO_2 showed an inferior 2,3-BDO conversion due to insufficient acid sites. Therefore, Cu/ZrO_2 and Cu/Al_2O_3 were employed for this reaction [88]. Though both catalysts exhibited promising acetoin selectivity, Cu/ZrO_2 performed better due to its lower acid site strength and number, which otherwise could catalyse side reactions for $Cu-Al_2O_3$ [88]. However, acetoin selectivity decreased steadily with increasing reaction temperatures, as higher temperatures favoured diacetyl formation [88]. Zn-Cr and V-Mg oxides are other catalysts explored for 2,3-BDO dehydrogenation, and both catalysts showed good selectivity to acetoin and diacetyl, but 2,3-BDO conversion remained low even at high temperatures [89].

Butylenes. Butylenes are important building-block chemicals for manufacturing a range of polymers [90]. Butylenes formation comprises 2,3-BDO dehydration over acidic sites to MEK/IBA, followed by their hydrogenation on metal sites to butanol, which is dehydrated to butylenes [91]. The copper-supported solid-acid catalysts are thus used in this reaction (Table 9). For Cu/ZSM5 catalyst, butylenes selectivity was increased with increasing Si/Al and H_2/2,3-BDO ratios [92]. A high H_2/2,3-BDO ratio favours hydrogenation reaction, while the high Si/Al ratio, i.e., low acidity, inhibits coke formation with high olefin selectivity [92]. The balance between Cu content and acidity is thus crucial for high butylene selectivity [93]. Conversely, V/SiO_2 offers both weakly acidic sites for dehydration reaction and polymeric Vox species for transfer hydrogenation of MEK from 2,3-BDO [94]. V/SiO_2 thus showed the highest butylenes selectivity of 45.2% in the absence of hydrogen at 500 °C [94]. In another study, bifunctional Cu-modified 2D pillared MFI zeolite was employed to produce butylene-rich C_{3+} olefins. Cu/PMFI exhibited better C_{3+} olefins selectivity than Cu/ZSM-5 due to the inhibition of coke formation [90]. The short diffusion length minimized non-butene C_{3+} olefins formation by inhibiting their further conversion via oligomerization and cracking reactions [90]. The mesoporous catalyst was also reported to suppress cracking reactions with improved catalyst stability [91].

3.2. 1,4-Butanediol (1,4-BDO)

Tetrahydrofuran (THF). THF holds applications as an industrial solvent and precursor for polyurethanes, elastic fibers, and several organic chemicals [95]. It is manufactured by acid-catalyzed dehydration of 1,4-BDO (Fig. 6) [96]. Experimental and *in situ* DRIFTS study using Yb/Zr catalyst demonstrated that -OH groups interact with acidic sites while β-H abstraction occurs on basic sites (Fig. 5) [97]. The reaction was thus favorable to THF over strong acidic sites; however, high basic/acid site density turned the reaction towards 3-buten-1-ol (3B1OL). Various solid-acid catalysts, such as γ-Al_2O_3, heteropolyacids, zeolites, and acidic resins, were thus investigated for this reaction (Table 10). γ-Al_2O_3 and Yb/SiO_2 possess weak Lewis acid sites, and the elevated reaction temperature is thus needed for high 1,4-BDO conversion with good THF selectivity [13,98]. Zeolites are other solid-acid catalysts with microporous structures. The commercial zeolites showed more than 99% selectivity to THF in liquid-phase 1,4-BDO dehydration [99]. However, H^+ or NH_4^+ forms exhibited higher 1,4-BDO conversion than Na^+ forms due to their stronger acidity. Besides, the catalytic activity of small-pore Ferrierite was lowest due to diffusion restriction of THF. However, medium-pore ZSM-5 showed the highest catalytic activity, followed by large-pore Y, Mordenite, and Beta. Further, liquid phase 1,4-BDO dehydration was investigated using 4.6 wt% CuO-modified nano ZSM-5 in a rotary evaporator with continuous removal of THF and water from the reactor [100]. The synergetic interaction between CuO and ZSM-5 was responsible for its high acidity, with almost 100% 1,4-BDO conversion and THF selectivity.

The kinetics of the liquid phase 1,4-BDO dehydration was studied over cation exchange resins with strong Brønsted acidity at lower temperatures due to its thermal stability limitations [96,101]. Though cation exchange resin was highly selective to THF, 1,4-BDO conversion remained low due to low reaction temperature. The water was reported to have detrimental effects on the reaction rate due to competing absorption of -OH groups from solvent and 1,4-BDO on acidic sites, resulting in poor 1,4-BDO conversion. For liquid-phase 1,4-BDO dehydration, heteropoly acid (tungsten-substituted molybdophosphoric acids) showed nearly 97% 1,4-BDO conversion within the first 15 min, with almost 100% selectivity to THF [102]. The catalytic activity was further improved with increased tungsten content due to enhanced acidity.

3-Buten-1-ol (3B1OL). 3B1OL is used to synthesize many functional polymers and heterocyclic drugs, such as multidrug-resistant compounds, antiproliferative, antiviral, and antitumor agents [34–36]. Pure ZrO_2 showed poor 3B1OL selectivity owing to the lack of strong basicity for β-H abstraction (Table 11 and Fig. 5) [103]. Though alkali (Li, Na, and K) and alkaline earth (Ca, Ba, and Sr) metal oxides-modified ZrO_2 improved basic sites with enhanced 3B1OL selectivity; they showed slightly lower acidity with reduced 1,4-BDO conversion [104,105]. On the contrary, owing to a suitable ionic radius, Ca^{2+} can easily enter the ZrO_2 lattice forming Ca–O–Zr surface species accompanied by the evolution of new acidic sites compared to alkali metal and other alkaline earth metal (SrO and BaO) oxides [104,106,107]. Besides, SrO and BaO react with ZrO_2 forming zirconate, accompanied by a reduction in acidic sites. The CaO-modified ZrO_2 thus demonstrated the best catalytic performance. CeO_2 is another metal oxide with redox properties and basicity. These characteristics make pure ceria highly selective

to 3B1OL with reasonable 1,4-BDO conversion at the moderate reaction temperature [108,109]. However, ceria exhibits a surface-structure sensitive characteristics, with dominant catalytically active (1 1 1) facets on large ceria particles [110]. The catalytic activity and 3B1OL selectivity were thus enhanced with increasing ceria particle size with the maximum at 65.0 nm [111]. The reaction was further studied over bulk and ZrO_2-supported REO [82,112]. The weakly basic heavier REOs were more selective towards 3B1OL, while strongly basic lighter REOs were selective towards THF and GBL. The surface acid-base properties of REO were regulated by their geometry, affecting the UOL selectivity [112]. In addition, Mg-Yb oxide showed good catalytic performance in 1,4-BDO dehydration with high 3B1OL selectivity [113].

1,3-Butadiene (BD). 1,4-BDO dehydration involves three competing reactions: (i) cyclodehydration to THF, (ii) single dehydration to 3B1OL, and (iii) double dehydration to BD (Fig. 6). Generally, the reaction is highly selective to THF over solid-acid catalysts at moderate reaction temperature (250-320 °C) under the liquid phase [66]. The slightly higher reaction temperatures under the vapor phase turn the reaction towards 3B1OL, with an insignificant amount of BD. However, BD becomes the dominant product beyond 400 °C. Further, it has been proposed that the single dehydration and cyclodehydration products convert directly to BD beyond 360 °C [114].

γ-Al_2O_3 and SiO_2-Al_2O_3 showed good BD selectivity at relatively lower temperatures at the expense of low 1,4-BDO conversion (Table 12) [13]. However, the BD selectivity dropped drastically at higher reaction temperatures, with THF as the major product. Besides, SiO_2-Al_2O_3 deactivated rapidly under reaction conditions [115]. However, Ag-modified SiO_2-Al_2O_3 showed improved catalytic stability for 3B1OL dehydration to BD [115]. The vapor-phase reaction was further studied using various rare earth zirconates [116]. Among these, $Y_2Zr_2O_7$ and $Dy_2Zr_2O_7$ displayed promising catalytic performance. However, the product selectivity was closely related to the reaction temperature and WHSV [116]. 1,4-BDO conversion and BD selectivity were enhanced steadily with rising reaction temperature, with a simultaneous drop in THF selectivity, reaching close to 80% BD selectivity and complete 1,4-BDO conversion at 350 °C [109,116,117]. However, the propylene became significant at elevated temperatures since the decomposition of 3B1OL was favoured at high temperatures by the retro-Prince reaction [116]. Besides, the selectivity of UOL and THF was decreased with decreasing WHSV, with an equivalent increase in BD selectivity [118]. These results demonstrated that the intermediate UOL and THF were converted to BD at elevated temperatures and longer space-time. In another study, ionic liquid (tetrabutylphosphonium bromide) was found to be effective for 1,4-BDO dehydration even at a low reaction temperature of 200 °C, with more than 94% BD yield [114].

γ-**Butyrolactone (GBL).** GBL is the simplest 4-carbon lactone used as an industrial solvent and intermediate for manufacturing medicines, fibers, and pesticides [119]. GBL can be produced from 1,4-BDO by two different reaction routes: (i) dehydrocyclization and (ii) catalytic oxidation [119,120]. The Cu-based catalysts have been widely used for vapor-phase dehydrocyclization of 1,4-BDO due to their high catalytic activity and GBL selectivity, with only a small amount of 2,3-dihydrofuran and THF (Table 13). However, 12 wt% Cu/SiO_2 deactivated rapidly due to the sintering of Cu at elevated temperatures and partial oxidation of catalytically active

metallic Cu [120]. The alkali (Na) and alkaline earth (Ca) metal oxides were thus introduced to retard the agglomeration of Cu with a slight improvement in catalyst stability. However, GBL selectivity remained lower than unmodified Cu/SiO$_2$ due to the strong basic sites [120]. The reaction under hydrogen flow is another strategy for the *in-situ* regeneration of metallic Cu^0 from catalytically inactive Cu$^+$ and Cu^{2+}. Though this approach successfully achieved stable catalytic performance of alkali-modified Cu/SiO$_2$ for 100 h time-on-stream, however, GBL selectivity remained low owing to strong basicity. 80 wt% Cu/SiO$_2$ nanocomposite was thus proposed to overcome these challenges [120]. The agglomeration of Cu was suppressed due to the addition of silica nanoparticles between copper nanoparticles. This catalyst thus showed stable catalytic performance for 400 h time-on-steam, with around 99% 1,4-BDO conversion and 99% GBL selectivity.

In another study, 5-6 wt% alkaline earth metal (Ba, Ca, Sr, and Mg)-modified 30-35 wt% Cu/SiO$_2$ was employed for vapor phase 1,4-BDO dehydrocyclization [121]. The Cu$^+$ and Cu^{2+} species were Lewis acidic, which were neutralized by alkaline Ca, Sr, and Ba metal oxides. Therefore, Ca, Sr, and Ba-modified Cu/SiO$_2$ showed better 1,4-BDO conversion and GBL selectivity than Cu/SiO$_2$. Especially, Ba-modified Cu/SiO$_2$ showed 99.6% GBL yield even at 900 h time-on-stream. However, new acidic sites were evolved by Mg doping, with lower 1,4-BDO conversion and GBL selectivity than Cu/SiO$_2$. The effect of supports (MgO, γ-Al$_2$O$_3$, MgO–Al$_2$O$_3$, and SiO$_2$) for 10 wt% Cu catalysts was evaluated for 1,4-BDO dehydrocyclization reaction [122]. While all other catalysts exhibited around 99% 1,4-BDO conversion, inferior catalytic activity was observed over Cu/MgO–Al$_2$O$_3$ due to poor metal dispersion. Cu/MgO and Cu/SiO$_2$ primarily catalysed the dehydrogenation reaction due to the absence of acidic sites, with 99% GBL selectivity. However, acidic sites of alumina favoured dehydration reaction, with >90% THF selectivity over Cu/MgO–Al$_2$O$_3$ and Cu/Al$_2$O$_3$ catalysts. Though low concentration (1 wt%) of promoters (Co$_3$O$_4$, Cr$_2$O$_3$, and ZnO) were ineffective, 10 wt% promoters in 20 wt% Cu/MgO improved catalytic activity significantly [123].

The dehydrocyclization releases two moles of hydrogen per mole of 1,4-BDO. Therefore, several studies proposed coupling this reaction with hydrogenation to utilize the generated hydrogen. 1,4-BDO dehydrocyclization was successfully coupled with maleic anhydride hydrogenation over Cu-Zn-Al catalyst [124], acetophenone hydrogenation over supported Cu catalyst [122], nitrobenzene hydrogenation over Co$_3$O$_4$, Cr$_2$O$_3$, and ZnO-promoted Cu/MgO catalyst [123], and benzaldehyde hydrogenation over Cu/CeO$_2$-Al$_2$O$_3$ [125]. The catalytic oxidation of 1,4-BDO under the liquid phase was studied over Au/TiO$_2$, Au/SnO$_2$, and Au/Fe-Al-O composite catalysts [119,126,127]. 8 wt% Au/TiO$_2$ with 573–673 Kcalcination temperature resulted in better metal dispersion, with 99% 1,4-BDO conversion and almost 100% GBL selectivity at relatively mild reaction conditions [119].

3.3 1,3-Butanediol (1,3-BDO)

1,3-BDO dehydration produces BD via UOLs intermediates, while 3-HBAD is obtained via dehydrogenation of 1,3-BDO (Fig. 7). Among REO, CeO$_2$ showed the best UOL selectivity (Table 14) [128]. CeO$_2$ was further modified using Fe, Ni, and Co oxides to generate additional redox sites. However, 1,3-BDO conversion was

lower for Fe and Co-modified CeO_2 than pure CeO_2 [128]. The weakly basic heavier REOs, such as Y_2O_3 and Yb_2O_3, showed high selectivity to UOL, while strongly basic lighter REOs catalyzed 1,3-BDO oxidation to propanone, butanone, MEK, etc. [129]. Though 3B1OL was the major product over ZrO_2, it resulted in a wide range of products [130]. Besides, 1,3-BDO conversion remained low due to its weak acidity [130]. However, Yb_2O_3-ZrO_2 mixed metal oxide showed good UOL selectivity [118].

H-ferrierite (Si/Al = 130) having medium-pore diameter for easy diffusion of molecules and ZSM-5 (260) with Bronsted acid sites and medium acidic strength showed a high BD selectivity [131,132]. However, zeolites showed 3B1OL as a major by-product due to its extra stability, which prevents further dehydration [132]. However, mesoporous Al-SBA-15, with dominant weaker Lewis acid sites, converted UOL to BD efficiently [131]. However, it showed a significant amount of propylene, with slightly lower BD selectivity than ZSM-5.

4-Hydroxy-2-butanone (4H2B) is used as a precursor to produce pesticides, steroids, and anticancer drug doxorubicin [47,133]. The vapor phase dehydrogenation of 1,3-BDO to 4H2B was carried out over CuO and Cu/ZnO; however, 1,3-BDO conversion was low (Table 15) [134]. Though Al_2O_3 and ZrO_2-modified CuO improved 1,3-BDO conversion, 4H2B selectivity was dropped due to 4H2B dehydration to 2-buten-2-one, followed by hydrogenation to butanone [134]. Moreover, basic Cu/MgO catalyzed retro-aldol reaction forming 4H2B to form formaldehyde and propanone [134]. The liquid phase 1,3-BDO oxidation to 3-hydroxybutyric acid (3-HBA) was also explored over $PtSb_2$ alloy [135]. This alloy promoted tandem oxidation of 3-HBAD to 3-HBA with minimum side reactions.

4. Examples showcasing catalytic upgrading of bio-based C4 diols

The growing interest in sustainability and committed efforts towards decarbonisation have realised the commercialization of bio-based BDOs. In the last decade, a few research groups and industries have demonstrated the upgradation of bio-based BDOs to various chemicals and fuels using integrated fermentation and chemo-catalysis approaches, as showcased in this section.

In the year 2016, bio-based 2,3-BDO obtained by glucose fermentation using *Zymobacter palmae* was upgraded to BD [86]. 2,3-BDO was purified from fermentation broth sequentially by microfiltration, nanofiltration, and ion exchange, followed by concentration using a film evaporator. 2,3-BDO was then subjected to vapor-phase dehydration (N_2: 30 ml/min, temperature: 401-404°C, time-on-stream: 8 h) using the silica-supported cesium dihydrogen phosphate catalyst in a fixed-bed reactor. The bio-based 2,3-BDO showed almost complete conversion and BD selectivity (91.9%) as high as that of fossil-based 2,3-BDO, despite the presence of impurities and water [86].

The US Department of Energy, in their first attempt, demonstrated catalytic conversion of simulated 2,3-BDO broth to C3+ olefins, followed by oligomerization and hydrogenation to produce sustainable aviation fuel [136]. 2,3-BDO was converted to C3+ olefins using Cu/ZSM-5 catalyst at 250°C, with ~97% 2,3-BDO conversion and 95-98% selectivity in 41 h time-on-stream. 2,3-BDO conversion, selectivity of C3+ olefins, and catalyst stability remained unaffected by co-feeding 10% acetoin or 40% water with 2,3-BDO. However, co-feeding 10%

acetic acid reduced the selectivity of olefins (95% to 73%) with enhanced coke formation. This study suggested that organic acids like acetic acid could be detrimental to the catalysts, indicating the importance of removing acidic metabolites before their catalytic conversion.

Recently, Affandey et al. used fermentation broth containing 10 wt% 2,3-BDO as feedstock to obtain sustainable aviation fuel [137]. 2,3-BDO was first produced from sugar-rich hydrolysates derived from corn stover. The feedstock was subjected to deacetylation and mechanical refining, followed by hydrolysis using Cellic Ctec2/Htec2 blend. Later, corn stover hydrolysate was subjected to microfiltration and vacuum evaporation to generate a concentrated sugar solution containing 287 g/L glucose and 136 g/L xylose as predominant sugars. A fed-batch fermentation strategy was devised wherein a recombinant and sugar co-fermenting *Zymomonas mobilis* was used for 2,3-BDO production in a 160 L bioreactor, yielding 90 g/L 2,3-BDO, with acetoin and glycerol as by-products along with residual sugars, proteins, and salts as other broth constituents. Before catalytic upgrading, the cell-free pre-filtered fermentation broth was subjected to nanofiltration using NF95 membrane to remove the impurities, which led to 41% loss of 2,3 BDO. The catalytic upgrading of 2,3-BDO to aviation fuel was carried out in four sequential steps: production of (i) MEK from 2,3-BDO using $AlPO_4$ and (ii) olefins from MEK using $Zn_1Zr_{10}O_x$, followed by (iii) oligomerization of olefins using zeolite beta and (iv) hydrogenation of oligomers over platinum/carbon to jet fuel blend stock. However, despite removing impurities from fermentation broth to a large extent, the MEK formation catalyst showed a continuous conversion loss due to deactivation steaming from feed impurities. The characterization study using two-dimensional GC X GC confirmed the presence of 31.7 wt% isoalkanes, 29.6 wt% cycloalkanes, and 24.5 wt% n-alkanes in aviation fuel blend stock. However, the specification of the final distilled product differed from ASTM D7566 specifications, implying a need for process improvements in the near future.

Likewise, in 2023, 2,3-BDO produced by fermentation of corn stover hydrolysate was selectively separated and upgraded to 1,3-dioxolane using reactive extraction with butyraldehyde, which could be easily separated by decantation [138]. In this experiment, the fermentation broth was subjected to metal ion (Na, K, Ca, and Mg) removal using Dowex50WX8 to avoid negative interference on Nafion N50R catalyst during recycling. The optimum conditions of reactive extraction, which yielded >95% 1,3-dioxolane, were 10 wt% catalyst, 40°C, 5 h, and 1:5 2,3-BDO/butyraldehyde. This dioxolane can be directly used as an ignition fuel. The authors further devised a strategy wherein dioxolane was treated with methanol in the presence of Nafion N50R to obtain high purity 2,3-BDO by trans-acetalization or alternately could be cleaved to butyraldehyde and MEK using ZSM-5 catalyst. This process was granted a US patent on 31Jan 2023 (US 11,565,989B2).

5. Challenges

Fermentative production of C4 diols gained significant interest owing to their environmental friendliness and massive derivatives market. Developing cost-effective bio-based processes is thus extremely important for the sustainability of the petrochemical sector. However, integrated bio- and chemo-catalytic approaches are yet to be commercialized for producing valuable products, except few attempts by some research groups [13,137,139].

Even in current times, the market share of fermentative C4 alcohols is quite less and limited to only a few of them, while most of them are under development due to inefficient bioprocess with prohibitive production prices [15]. However, there are four bio-based marketable technologies for 2,3-BDO and one commercial technology by Genomatica for 1,3-BDO and 1,4-BDO [45,140]. Despite tremendous research efforts and commercial adventures, significant challenges still exist in the biosynthesis of C4 diols and their derivatization via chemo-catalysis, as discussed below.

5.1. High feedstock cost

Cheap manufacturing is the deciding factor for the success of commercialization, which is only possible with high TYP metrics, low-cost substrate, and inexpensive downstream processing. The feedstock cost alone accounts for 25-50% of the selling price. Therefore, the use of low-cost biomass wastes from the agro-industrial sector across the supply chain should be encouraged that do not compete with food and feed industries [141]. However, these crude feedstocks often require energy-intensive preprocessing accompanied by the formation of fermentation inhibitors retarding microbial performance. Thus, most industrial strains fail to perform as per expectations with non-edible and waste biomass. Therefore, an additional unit operation, detoxification, is required, which though does not guarantee the same performance as pure sugars [142]. As the impetus is growing for using alternative carbon sources, more efforts are needed to design robust strains to assimilate crude renewable sources with the same ease as pure carbon sources [143].

5.2. TYP metrics

Industrial viability can only be envisaged with high production levels in terms of titer, yield, and productivity. Recent advances in metabolic engineering and synthetic biology enabled significant progress in efficient BDO production [10,23,49]. The microbial 2,3-BDO production is promising in terms of fermentation parameters, such as titer >100 g/L and yield close to the theoretical one (0.50 g/g). Usually, productivity above 2.0 g/L.h is required for economic viability and to compete with petroleum-based processes. However, low productivity (<2.0 g/L.h) of 2,3-BDO by non-pathogenic strains has been speculated as one of the hurdles in bulk production as lower productivity requires large capacity, which incurs extra operational costs [31,144]. For example, the volumetric productivity of commercial production of 1,3-propanediol by DuPont is 3.5 g/L.h [145]. On the other hand, 1,3-BDO and 1,4-BDO are the non-natural metabolites, where 1,4-BDO is commercially produced via the biological route, while titer of 1,3-BDO stays under 30 g/L, and TYP metrics are far from industrial manufacturing. Currently, Genomatica, a US-based company, and GS Caltex, an oil refinery company in South Korea, are the active players in commercial bio-based production of 1,4-BDO and 2,3-BDO, respectively [15].

5.3. Continuous supply of reducing equivalents

The diols are reduced products and tightly coupled with the NAD(P)H/NAD(P)$^+$ratio. The production of one mole of 2,3-BDO, 1,3-BDO, and 1,4-BDO requires the consumption of 2, 3, and 4 moles of NAD(P)H, respectively (Fig. 1 and Fig. 2). In other words, a high-level production cannot be achieved without a continuous supply of reducing power to drive the smooth production. In cellular metabolism, the TCA cycle is a major source

of reducing power, also required for cell growth for energy generation, and this leads to competition between biomass and product formation. The high flux through the TCA cycle under microaerobic or anaerobic conditions favours diols formation, which contradicts with cellular growth proliferation requiring high oxygen levels. The challenge is to divert maximal carbon and reducing power towards the efficient synthesis of BDO, and one of the solutions could be aerobic-anaerobic switching cultivation like ethanol production by *Saccharomyces cerevisiae* [49]. Greater availability of cofactors could be secured by cofactor engineering to enhance reducing power by introducing/amplifying biochemical reactions generating NAD(P)H and/or those consuming reducing equivalents. For example, formate dehydrogenase has been used to generate extra NADH with an exogenous supply of formate [Formate + NAD^+ → CO_2 + NADH], i.e., the introduction of FDH from *Candida boidinii* in *Klebsiella oxytoca* [146,147]. The cofactors could be manipulated to enhance their levels to favour the desired reactions. Transhydrogenase inter-converting NADH to NADPH and vice versa can be exploited to elevate the concentration of the required cofactor [148]. For example, the production of 1,3-BDO was enhanced through overexpression of *pntAB* encoding for a membrane-bound proton-translocating transhydrogenase.

5.4. Carbon loss

The formation of C4 diols starts with the decarboxylation of pyruvate, accompanied by the loss of carbon in the form of CO_2 [149]. In fact, one-third of substrate carbon is lost during the production of these diols, restricting their yields. For example, in the case of glucose as starting material, the theoretical yield of diol is 0.50 g/g [$C_6H_{12}O_6$ → $C_4H_{10}O_2$ + $2CO_2$], affecting the process economics. The CO_2 released during fermentation can be captured instead of released into the atmosphere and channelised towards BDO production [14]. For example, Guadalupe-Medina et al. overexpressed Calvin cycle enzymes [phosphoribulokinase (PRK) and ribulose-1,5-bisphosphate carboxylase (Rubisco)] to reuse CO_2 released during ethanol production back into central carbon metabolism [150]. The calculation shows that if the CO_2 is recirculated without being lost, the theoretical maximum yields of BDO from glucose can improve from 1 mol BDO/mol glucose (0.50 g/g) to 1.5 BDO mol/mol glucose (0.75 g/g). The carbon loss limitation can also be mitigated by using CO_2-fixing bacteria such as photoautotrophs and lithoautotrophs. Besides, the CO_2 can also be fixed by applying designed synthetic *in vitro* systems [147], or its fixation efficiency can be increased by rationally engineering enzymes for improved carboxylation [148]. At the same time, the carbon loss can be reduced through pathway engineering [145] or the use of a mixotroph [149,150]. The strategies based on enzyme, pathways, or process engineering can significantly improve TYP metrics, reduce the cost burden, and make it competitive with fossil-based production.

5.5. Lengthy non-native metabolic pathways

2,3-BDO is a natural product and is formed from pyruvate via three-step reactions. In the case of naturally producing strains, the work does not start from scratch and is acquired with better resistance for the product, which is not guaranteed in the case of non-native strains [147]. Unlike 2,3-BDO, 1,3-BDO and 1,4-BDO are non-native products with synthetic pathways containing multiple heterologous enzymes catalysing non-natural substrates. Since these pathways are not part of cellular metabolism, and drain out the flux from natural carbon

flow towards non-native products, imposing a metabolic burden on the cell. Therefore, cells need to be adapted to these pathways to synchronize with native metabolism to run them efficiently. The enhanced performance can be achieved with chemo-informatic, enzyme engineering, and directed evolution approaches for better understanding and improving the substrate promiscuity of native and engineered enzymes [49].

5.6. End-product toxicity

The productivity of microbial fermentation often declines during later stages after accumulating a significant amount of end-product. The situation is exacerbated along with the accumulation of other unwanted by-products, and the inhibition resulting from the product sets a maximum attainable limit on titer [151]. At higher concentrations, the end-product moves from the extracellular medium to the inside of the cell, and the reverse reaction also become active [148,152]. The negative impacts caused by end-product toxicity and multiple product inhibition need to be overcome, and strategies in this direction rely on evolutionary engineering techniques, random mutagenesis, and the underlying mechanism involved are not known. Instead, the focus should be on the rationally designed evolution of strains and key enzymes to develop more tolerant strains with the aid of genomic and omics analysis [143]. The other solution could be the transport engineering approach with the use of efflux pumps, modification of export proteins, membrane composition, and/or *in situ* removal of product before reaching the stage when the product is amassed in higher amounts [152,153].

5.7. Expensive product recovery

Downstream processing (DSP) is one of the major contributors to the overall share and plays a decisive role in minimal selling price (MSP). Therefore, economical product recovery is the most important aspect of bioprocessing. The final output of DSP also governs the conversion efficiency and product selectivity during chemical upgradation. The complexity of DSP of C4 diol arises from their high boiling points (>170 ^{0}C, Table 1) and high hydrophilicity, making their separation from aqueous broth energy-intensive via distillation [14]. Similarly, their separation via solvent extraction is challenging due to their high hydrophilicity and densities close to water. Further, fermentation generates various by-products in the form of organic acids and alcohols and contains unconsumed nutrients, such as sugars, proteins, etc., making fermentation broth a complex mixture [141]. These unwanted metabolites and residual nutrients added to the fermenter make the separation of the C4 diols complex. Several schemes based on the conventional distillation, hybrid extraction-distillation process, or aqueous two-phase system have been developed for 2,3-BDO recovery [27,154,155]. However, the recovery of 1,3-BDO and 1,4-BDO remains a significant challenge [13,48]. The situation is further exacerbated by low solvent titers, such as, in the case of 1,3-BDO. Advanced separation strategies, such as membrane separation, adsorption, hybrid distillation-extraction, membrane-distillation, etc., should be developed to reduce energy consumption and operational costs [51].

5.8. Robust catalysts for direct conversion of fermentative BDOs

Most of the chemo-catalytic upgrading of C4 diols employed pure or analytical grade chemicals. However, these catalysts fail to perform when the same optimized processes are evaluated using simulated or real-time

fermentation broth containing C4 diols. These differences are due to the impurities present in the fermentation broth, such as biomass residues, inorganic nutrients, and other metabolites, that negatively impact the performance, stability, product selectivity, and reusability of the catalyst [136–138,156]. The robustness of chemical catalysts is thus a pre-requisite for efficient amalgamation with bio-based processes so that they can withstand these impurities and can be repeatedly used without affecting the conversion, product selectivity, and yields. Therefore, robust catalysts that can work on fermentative BDOs should be developed to make C4 diol-based integrated biorefinery successful. The studies should be directed towards catalytic conversion of aqueous and fermentative BDOs to overcome these practical challenges. These challenges can be addressed by removing impurities by low-cost methods or developing robust catalysts with improved impurity tolerance. The impurity-tolerant catalysts can be envisaged using tailored supports or surface modifications with enhanced resistance to fouling, poisoning, and deactivation. The selection of the right collaborators/partners is also equally important for the successful execution of such interdisciplinary translation research. For instance, Genomatica focused primarily on developing robust engineered microbial factories which could produce industrially relevant titres of 1,4-BDO. However, for downstream product separation, they collaborated with Tate & Lyle Group, which already developed expertise in purifying 1,3-PDO while working with Dupont. As a result, their partnership could see the light of commercialization. Later, they licensed their technology to BASF, which is not only commercially producing bio-based 1,4-BDO but catalytically upgrading it to poly-THF, a primary material for making spandex fibers and a building block for producing polyurethanes [157].

5.9. Product selectivity in chemo-catalytic upgrading of C4 diol

The chemo-catalytic upgrading of C4 diols involves complex chemistry with thermodynamic and kinetic constraints. The C4 diols conversion pathways involve competing reactions, including dehydration, hydrogenation/hydrogenation, oxidation, esterification, and condensation [91]. Each reaction has its own set of catalysts and optimal reaction conditions. Therefore, developing catalysts for the selective transformation of C4 diol is one of the major hurdles. The C4 diol conversion often requires multiple functionalities (acid/base, metal, etc.) in the catalysts at their optimal density. Designing multifunctional catalysts with optimum functionality is thus crucial to improve carbon conversion to a high-value product while minimizing the by-products. Therefore, there is a need for a fundamental understanding of reaction mechanisms using computational modelling with experimental validation for rational catalyst design.

5.10. Catalyst stability

The reaction conditions, including high temperatures, pressures, and corrosive environments, can lead to the loss of catalyst activity over time. The feed impurities, reaction intermediates, and side products can further contribute to catalyst fouling and deactivation. Developing catalysts that exhibit long-term stability and resistance to deactivation is essential for developing economically viable continuous processes [73,74,82,134,158]. Extensive research is needed to understand catalyst deactivation using advanced catalyst characterization

techniques. Besides, optimizing process conditions and catalyst stability study in bench and pilot-scale are required to demonstrate their commercial suitability.

5.11. Non-inclusivity of techno-economic analysis (TEA) and life-cycle assessment (LCA)

The state-of-the-art reveals that most studies are research-oriented. However, TEA and LCA provide the techno-commercial-environmental perspectives of the overall process and are essential for translational research. These studies are specifically crucial for lignocellulosic biomass, as their composition is heterogeneous and varies with soil, weather, variety, geographical origin, etc., leading to inconsistent sugar titres during enzymatic hydrolysis. Further, these studies help decipher the major cost contributors and environmental hotspots that negatively impact sustainability. However, there are only a handful of studies on TEA of 2,3-BDO production from glycerol, sucrose, molasses, switch grass, brewer's spent grains, and sugarcane bagasse [19,159–161]. However, the TEA of production from corn-based dextrose [59] and Genomatica's GENO-BDO process are the only studies for 1,4-BDO. The latter showed that the reduction of water load in the process could lower the selling price by reducing the equipment size and cost, such as bioreactors, filtration systems, evaporators, distillation columns, etc. Furthermore, it has been proposed that the 1,4-BDO selling price can be reduced by 45% by increasing the current industrial 1,4-BDO titre to 280 g/L [56]. Similar to TEA, the LCA studies are limited. A further evaluation of commercial potential and process sustainability for bio-based BDOs production is required.

6. Conclusions

Highly functionalized BDOs inducted a new avenue for sustainable chemicals and fuels from biomass. This review presents the up-to-date status of the fermentative production of 2,3, 1,4, and 1,3-BDO from biomass and their chemo-catalytic conversion into various products. Significant progress has been made in microbial production of C4 diols in the last decade owing to advancements in synthetic biology and metabolic engineering for pathway design and strain optimization, especially for non-natural products, 1,3-BDO and 1,4-BDO. These diols are currently derived from petroleum, and they are the well-known precursors for the multitude of derivatives. The fermentative C4 diols are highly required to generate a spectrum of bio-based products to combat and mitigate multiple environmental problems, including carbon emission, accumulation of hazardous synthetic and non-degradable waste, and mismanagement of waste streams when climate crisis is potentially catastrophic. The multiple strategies, including pathway reconstruction, debottlenecking of rate-limiting steps, redox balancing, regulation of carbon flux at different branching nodes, by-products removal to channelize maximal carbon flux towards diol, efficient product transport, and reduction/elimination of end-product toxicity with continuous gaining knowledge about metabolic systems galvanize the design of powerful cell factories using intensive metabolic engineering and system and synthetic biology tools. Besides, process engineering approaches, such as the design of optimal cultivation, feeding, aeration, inexpensive product separation, and low-cost carbon sources, make bioprocess more economical and flexible to manufacturers to overcome geographical barriers in the availability of edible feedstock. These factors enhance the TYP metrics and make

them economically competitive with petrochemical routes, eventually leading to large-scale production of bio-based diols with reduced effort, time, and cost for establishing a sustainable chemical industry. Further, Government support through strict policies for using green chemicals and penalties for carbon emission will facilitate large-scale production of bio-diols and motivate research and development to improve bioprocess efficiency.

Fermentative BDOs introduced a new avenue for sustainable sources of fuels and chemicals by chemo-catalytic approaches, such as BD, MEK, THF, acetoin, diacetyl, GBL, 4H2B, etc., making it a potential platform chemical in biorefinery. However, multiple competing reactions and thermodynamic/kinetic limitations pose obstacles in the selective conversion of BDOs into chemicals. A proper balance of different active sites in the catalysts and optimal process conditions are vital in tuning the selectivity of a desired product. Significant theoretical and experimental studies are necessary for the fundamental understanding of reaction pathways and for designing multifunctional catalysts with high catalytic activity, product yield, and prolonged time-on-stream stability. Besides, instead of synthetic BDOs, extensive research initiatives should be directed towards demonstrating catalyst performance for chemo-catalytic conversion of fermentative BDOs. The integrated bio- and chemo-catalytic approach is now receiving global attention, and we believe that this review will trigger further research in this direction and will have the aptitude to influence the government policy and regulations to promote the biomanufacturing of products, which otherwise cannot be produced from biological routes alone. Therefore, it is anticipated that the integrated processes will be implemented in the near future to generate a spectrum of products, and it will increase steadily in the coming years, contributing sustainability to the chemical industry. Future research should also be directed towards techno-economic and environmental impact analysis of the integrated approach to evaluate their commercialization potential and environmental performance.

Abbreviations

BDO	Butanediol
BD	1,3-Butadiene
3B1OL	3-Buten-1-ol
3B2OL	3-Buten-2-ol
2B1OL	2-Buten-1-ol
CoA	coenzyme A
GBL	γ-Butyrolactone
4H2B	4-Hydroxy-2-butanone
3-HB-CoA	3-hydroxybutyryl-CoA
3-HBAD	3-hydroxybutyraldehyde
IBA	Isobutyraldehyde
MEK	Methyl ethyl ketone
REO	Rare earth oxides
THF	Tetrahydrofuran
UOL	Unsaturated alcohols
WHSV	Weight hourly space velocity

References

[1] V. Narisetty, R. Cox, N. Willoughby, E. Aktas, B. Tiwari, A.S. Matharu, K. Salonitis, V. Kumar, Sustain Energy Fuels 5 (2021) 4842–4849.

[2] V. Narisetty, R. Cox, R. Bommareddy, D. Agrawal, E. Ahmad, K.K. Pant, A.K. Chandel, S.K. Bhatia, D. Kumar, P. Binod, V.K. Gupta, V. Kumar, Sustain Energy Fuels 6 (2022) 29–65.

[3] E. Min, Chin J Catal 36 (2015) 1406–1408.

[4] S.K. Maity, Renewable Sustainable Energy Rev 43 (2015) 1427–45.

[5] S.K. Maity, Renewable Sustainable Energy Rev 43 (2015) 1446–1466.

[6] D. Sun, S. Sato, W. Ueda, A. Primo, H. Garcia, A. Corma, Green Chem 18 (2016) 2579–2597.

[7] J.J. Bozell, G.R. Petersen, Green Chem12 (2010) 539.

[8] Y.-S. Ko, J.W. Kim, J.A. Lee, T. Han, G.B. Kim, J.E. Park, S.Y. Lee, Chem Soc Rev 49 (2020) 4615–4636.

[9] S. Xie, Z. Li, G. Zhu, W. Song, C. Yi, J Clean Prod 343 (2022) 131033.

[10] S. Maina, A.A. Prabhu, N. Vivek, A. Vlysidis, A. Koutinas, V. Kumar, Biotechnol Adv 54 (2022) 107783.

[11] Y. Mori, S. Noda, T. Shirai, A. Kondo, Nat Commun 12 (2021) 2195.

[12] S. Rodgers, F. Meng, S. Poulston, A. Conradie, J. McKechnie, J Clean Prod 364 (2022) 132614.

[13] D. Sun, Y. Li, C. Yang, Y. Su, Y. Yamada, S. Sato, Fuel Process Technol 197 (2020) 106193.

[14] Y. Jiang, W. Liu, H. Zou, T. Cheng, N. Tian, M. Xian, Microb Cell Fact 13 (2014) 165.

[15] J.I. Yoo, Y.J. Sohn, J. Son, S.Y. Jo, J. Pyo, S.K. Park, J. Choi, J.C. Joo, H.T. Kim, S.J. Park, Biotechnol J 17 (2022) 2000451.

[16] J.W. Lee, M.-S. Han, S. Choi, J. Yi, T.W. Lee, S.Y. Lee, in: Comprehensive Biotechnology, Elsevier, 2011, 149–161.

[17] C.C. Satam, M.J. Realff, J Adv Manuf Process 2 (2020) e10054.

[18] H. Yim, R. Haselbeck, W. Niu, C. Pujol-Baxley, A. Burgard, J. Boldt, J. Khandurina, J.D. Trawick, R.E. Osterhout, R. Stephen, J. Estadilla, S. Teisan, H.B. Schreyer, S. Andrae, T.H. Yang, S.Y. Lee, M.J. Burk, S. Van Dien, Nat Chem Biol 7 (2011) 445–452.

[19] S. Mailaram, V. Narisetty, V. V. Ranade, V. Kumar, S.K. Maity, Ind Eng Chem Res 61 (2022) 2195–2205.

[20] https://www.chemanalyst.com/industry-report/butanediol-market-657.

[21] C. Li, M. Zhang, X. Di, D. Yin, W. Li, C. Liang, Chin J Catal 37 (2016) 1555–1561.

[22] V. Narisetty, L. Zhang, J. Zhang, C. Sze Ki Lin, Y. Wah Tong, P. Loke Show, S. Kant Bhatia, A. Misra, V. Kumar, Bioresour Technol 358 (2022) 127381.

[23] J. Cheng, J. Li, L. Zheng, J Agric Food Chem 69 (2021) 10480–10485.

[24] C.W. Song, J.M. Park, S.C. Chung, S.Y. Lee, H. Song, J Ind Microbiol Biotechnol 46 (2019) 1583–1601.

[25]   Y. Amraoui, A.A. Prabhu, V. Narisetty, F. Coulon, A. Kumar Chandel, N. Willoughby, S. Jacob, A. Koutinas, V. Kumar, Chem Eng J 427 (2022) 130851.

[26]   M. Köpke, C. Mihalcea, F. Liew, J.H. Tizard, M.S. Ali, J.J. Conolly, B. Al-Sinawi, S.D. Simpson, Appl Environ Microbiol 77 (2011) 5467–5475.

[27]   Y. Amraoui, V. Narisetty, F. Coulon, D. Agrawal, A.K. Chandel, S. Maina, A. Koutinas, V. Kumar, ACS Sustain Chem Eng 9 (2021) 10381–10391.

[28]   J.M. Park, C. Rathnasingh, H. Song, J Ind Microbiol Biotechnol 42 (2015) 1419–1425.

[29]   Y. Ge, K. Li, L. Li, C. Gao, L. Zhang, C. Ma, P. Xu, Green Chem18 (2016) 4693–4703.

[30]   Y. Qiu, J. Zhang, L. Li, Z. Wen, C.T. Nomura, S. Wu, S. Chen, Biotechnol Biofuels 9 (2016) 117.

[31]   J.W. Lee, Y.-G. Lee, Y.-S. Jin, C. V. Rao, Appl Microbiol Biotechnol 105 (2021) 5751–5767.

[32]   L. Johansen, K. Bryn, F.C. Stormer, J Bacteriol 123 (1975) 1124–1130.

[33]   R.J. Magee, N. Kosaric, Adv Appl Microbiol 32 (1987) 89–161.

[34]   Z. Xiao, P. Xu, Crit Rev Microbiol 33 (2007) 127–140.

[35]   S. Maina, E. Dheskali, H. Papapostolou, A.M. de Castro, D.M. Guimaraes Freire, G.J.E. Nychas, S. Papanikolaou, I.K. Kookos, A. Koutinas, ACS Sustain Chem Eng 9 (2021) 8692–8705.

[36]   Y. Liu, X. Cen, D. Liu, Z. Chen, ACS Synth Biol 10 (2021) 1946–1955.

[37]   https://www.marketwatch.com/press-release/2030-bio-based-13-butanediol-market-growth-future-prospects-and-competitive-analysis-2023-05-11 (accessed May 16, 2023).

[38]   T. Okabayashi, T. Nakajima, H. Yamamoto, US Patent No. US 2012/027660.6 A1, 2012.

[39]   A. Matsuyama, H. Yamamoto, N. Kawada, Y. Kobayashi, J Mol Catal B Enzym 11 (2001) 513–521.

[40]   N. Kataoka, A.S. Vangnai, T. Tajima, Y. Nakashimada, J. Kato, J Biosci Bioeng 115 (2013) 475–480.

[41]   N. Kataoka, A.S. Vangnai, H. Ueda, T. Tajima, Y. Nakashimada, J. Kato, Biosci Biotechnol Biochem 78 (2014) 695–700.

[42]   J. Wang, R. Zhang, J. Zhang, X. Gong, T. Jiang, X. Sun, X. Shen, J. Wang, Q. Yuan, Y. Yan, Green Chem23 (2021) 8694–8706.

[43]   K. Nemr, J.E.N. Müller, J.C. Joo, P. Gawand, R. Choudhary, B. Mendonca, S. Lu, X. Yu, A.F. Yakunin, R. Mahadevan, Metab Eng 48 (2018) 13–24.

[44]   T. Islam, T.P. Nguyen-Vo, V.K. Gaur, J. Lee, S. Park, Bioresour Technol 376 (2023) 128911.

[45]   https://www.genomatica.com/products/.

[46]   https://www.epa.gov/greenchemistry/green-chemistry-challenge-2020-greener-synthetic-pathways-award.

[47]   J.L. Gascoyne, R.R. Bommareddy, S. Heeb, N. Malys, Metab Eng 67 (2021) 262–276.

[48]   H. Liu, J.U. Bowie, Sci Rep 11 (2021) 9449.

[49] H. Guo, H. Liu, Y. Jin, R. Zhang, Y. Yu, L. Deng, F. Wang, Biochem Eng J 185 (2022) 108478.

[50] R. Gérardy, D.P. Debecker, J. Estager, P. Luis, J.C.M. Monbaliu, Chem Rev 120 (2020) 7219–7347.

[51] A. Burgard, M.J. Burk, R. Osterhout, S. Van Dien, H. Yim, Curr Opin Biotechnol 42 (2016) 118–125.

[52] https://www.verifiedmarketresearch.com/product/14-butanediol-market/ (accessed May 20, 2020).

[53] R.G.C. Silva, T.F. Ferreira, É.R. Borges, J Chem Technol Biotechnol 95 (2020) 3057–3070.

[54] N.R. Barton, A.P. Burgard, M.J. Burk, J.S. Crater, R.E. Osterhout, P. Pharkya, B.A. Steer, J. Sun, J.D. Trawick, S.J. Van Dien, T.H. Yang, H. Yim, J Ind Microbiol Biotechnol 42 (2015) 349–360.

[55] M.-Y. Wu, L.-Y. Sung, H. Li, C.-H. Huang, Y.-C. Hu, ACS Synth Biol 6 (2017) 2350–2361.

[56] V.D. Pham, S. Somasundaram, S.H. Lee, S.J. Park, S.H. Hong, Biotechnol Lett 38 (2016) 321–327.

[57] S. Kurihara, K. Kato, K. Asada, H. Kumagai, H. Suzuki, J Bacteriol 192 (2010) 4582–4591.

[58] http://www.genomatica.com/news/press-releases/successfulcommercial-production-of-5-million-pounds-of-bdo/).

[59] C.C. Satam, M. Daub, M.J. Realff, Biofuels Bioprod Biorefin 13 (2019) 1261–1273.

[60] H. Liu, T. Lu, Metab Eng 29 (2015) 135–141.

[61] J. Wang, R. Jain, X. Shen, X. Sun, M. Cheng, J.C. Liao, Q. Yuan, Y. Yan, Metab Eng 40 (2017) 148–156.

[62] Y.-S. Tai, M. Xiong, P. Jambunathan, J. Wang, J. Wang, C. Stapleton, K. Zhang, Nat Chem Biol 12 (2016) 247–253.

[63] L. Dai, C. Tai, Y. Shen, Y. Guo, F. Tao, Biocatal Biotransformation 37 (2019) 92–96.

[64] H. Zu, H. Zhang, A. Fan, J. Gu, Y. Nie, P. Luo, Y. Xu, Chin J Chem Eng 28 (2020) 2160–2166.

[65] A.D. Nguyen, I.Y. Hwang, O.K. Lee, D. Kim, M.G. Kalyuzhnaya, R. Mariyana, S. Hadiyati, M.S. Kim, E.Y. Lee, Metab Eng 47 (2018) 323–333.

[66] E. V. Makshina, M. Dusselier, W. Janssens, J. Degrève, P.A. Jacobs, B.F. Sels, Chem Soc Rev 43 (2014) 7917–7953.

[67] H. Duan, Y. Yamada, S. Sato, Appl Catal A Gen 491 (2015) 163–169.

[68] S. Thion, P. Diévart, P. Van Cauwenberghe, G. Dayma, Z. Serinyel, P. Dagaut, Proc Combust Inst 36 (2017) 459–467.

[69] F. Hoppe, U. Burke, M. Thewes, A. Heufer, F. Kremer, S. Pischinger, Fuel 167 (2016) 106–117.

[70] W. Kim, W. Shin, K.J. Lee, Y.S. Cho, H.S. Kim, I.N. Filimonov, Appl Catal A Gen 570 (2019) 148–163.

[71]   W. Zhang, D. Yu, X. Ji, H. Huang, Green Chem 14 (2012) 3441–3450.

[72]   B.A. Bekele, J. Poissonnier, J.W. Thybaut, J Catal 411 (2022) 200–211.

[73]   M.A. Nikitina, V.L. Sushkevich, I.I. Ivanova, Pet Chem 56 (2016) 230–236.

[74]   M.A. Nikitina, I.I. Ivanova, ChemCatChem 8 (2016) 1346–1353.

[75]   J. Zhao, D. Yu, W. Zhang, Y. Hu, T. Jiang, J. Fu, H. Huang, RSC Adv 6 (2016) 16988–
         16995.

[76]   D. Song, Ind Eng Chem Res 55 (2016) 11664–11671.

[77]   W. Kim, W. Shin, K.J. Lee, H. Song, H.S. Kim, D. Seung, I.N. Filimonov, Appl Catal A Gen
         511 (2016) 156–167.

[78]   H. Duan, D. Sun, Y. Yamada, S. Sato, Catal Commun 48 (2014) 1–4.

[79]   H. Duan, Y. Yamada, S. Sato, Appl Catal A Gen 487 (2014) 226–233.

[80]   H. Duan, Y. Yamada, S. Kubo, S. Sato, Appl Catal A Gen 530 (2017) 66–74.

[81]   F. Sato, S. Sato, Catal Commun 27 (2012) 129–133.

[82]   S. Sato, R. Takahashi, M. Kobune, H. Inoue, Y. Izawa, H. Ohno, K. Takahashi, Appl Catal A
         Gen 356 (2009) 64–71.

[83]   X. Liu, V. Fabos, S. Taylor, D.W. Knight, K. Whiston, G.J. Hutchings, Chem - Eur J 22
         (2016) 12290–12294.

[84]   F. Zeng, W.J. Tenn, S.N.V.K. Aki, J. Xu, B. Liu, K.L. Hohn, J Catal 344 (2016) 77–89.

[85]   N.T.T. Nguyen, F. Matei-Rutkovska, M. Huchede, K. Jaillardon, G. Qingyi, C. Michel, J.M.M.
         Millet, Catal Today 323 (2019) 62–68.

[86]   D. Tsukamoto, S. Sakami, M. Ito, K. Yamada, T. Yonehara, Chem Lett 45 (2016) 831–833.

[87]   E. Yuan, P. Ni, J. Xie, P. Jian, X. Hou, ACS Sustain Chem Eng 8 (2020) 15716–15731.

[88]   Z. Al-Auda, X. Li, K.L. Hohn, Ind Eng Chem Res 61 (2022) 3530–3538.

[89]   H.U. Blaser, A. Baiker, R. Prins, Heterogeneous Catalysis and Fine Chemicals IV, Academic
         Press, Elsevier, 1997, 415-420.

[90]   S. Adhikari, J. Zhang, K. Unocic, E.C. Wegener, P. Kunal, D.J. Deka, T. Toops, S. Sinha
         Majumdar, T.R. Krause, D. Liu, Z. Li, ACS Sustain Chem Eng 10 (2022) 1664–1674.

[91]   Q. Zheng, J. Grossardt, H. Almkhelfe, J. Xu, B.P. Grady, J.T. Douglas, P.B. Amama, K.L.
         Hohn, J Catal 354 (2017) 182–196.

[92]   Q. Zheng, M.D. Wales, M.G. Heidlage, M. Rezac, H. Wang, S.H. Bossmann, K.L. Hohn, J
         Catal 330 (2015) 222–237.

[93]   Q. Zheng, J. Xu, B. Liu, K.L. Hohn, J Catal 360 (2018) 221–239.

[94]   K.M. Kwok, C.K.S. Choong, D.S.W. Ong, J.C.Q. Ng, C.G. Gwie, L. Chen, A. Borgna,
         ChemCatChem 9 (2017) 2443–2447.

[95]   Industrial Organic Chemicals: Starting Materials and Intermediates., Wiley-VCH, 1999.

[96]   V.M. Shinde, G.N. Patil, A. Katariya, Y.S. Mahajan, Chemical Engineering and Processing:
         Process Intensification 95 (2015) 241–248.

[97]   R. Mi, Z. Hu, B. Yang, J Catal 370 (2019) 138–151.

[98] T. Yamamoto, T. Matsuyama, T. Tanaka, T. Funabiki, S. Yoshida, Phys Chem Chem Phys 1 (1999) 2841-2849.

[99] M. Aghaziarati, M. Kazemeini, M. Soltanieh, S. Sahebdelfar, Ind Eng Chem Res 46 (2007) 726–733.

[100] Y. Long, S. Liu, Y. Fei, Q. Li, Y. Deng, Sci China Chem 60 (2017) 964–969.

[101] U. Limbeck, C. Altwicker, U. Kunz, U. Hoffmann, Chem Eng Sci 56 (2001) 2171–2178.

[102] H. Wu, M. Zhou, Y. Qu, H. Li, H. Yin, Chin J Chem Eng 17 (2009) 200–206.

[103] N. Yamamoto, S. Sato, R. Takahashi, K. Inui, Catal Commun 6 (2005) 480–484.

[104] N. Yamamoto, S. Sato, R. Takahashi, K. Inui, J Mol Catal A Chem 243 (2006) 52–59.

[105] Q. Zhang, Y. Zhang, H. Li, Y. Zhao, M. Ma, Y. Yu, Chin J Catal 34 (2013) 1159–1166.

[106] H. Duan, T. Hirota, S. Ohtsuka, Y. Yamada, S. Sato, Appl Catal A Gen 535 (2017) 9–16.

[107] Q. Zhang, Y. Zhang, H. Li, C. Gao, Y. Zhao, Appl Catal A Gen 466 (2013) 233–239.

[108] S. Sato, R. Takahashi, T. Sodesawa, N. Honda, J Mol Catal A Chem 221 (2004) 177–183.

[109] S. Sato, R. Takahashi, T. Sodesawa, N. Yamamoto, Catal Commun 5 (2004) 397–400.

[110] M. Kobune, S. Sato, R. Takahashi, J Mol Catal A Chem 279 (2008) 10–19.

[111] Y. He, Q. Li, Y. Wang, Y. Zhao, Chin J Catal 31 (2010) 619–622.

[112] H. Inoue, S. Sato, R. Takahashi, Y. Izawa, H. Ohno, K. Takahashi, Appl Catal A Gen 352 (2009) 66–73.

[113] R. Mi, Z. Hu, C. Yi, B. Yang, ChemCatChem 12 (2020) 2859–2871.

[114] M. Stalpaert, F.G. Cirujano, D.E. De Vos, ACS Catal 7 (2017) 5802–5809.

[115] D. Sun, S. Arai, H. Duan, Y. Yamada, S. Sato, Appl Catal A Gen 531 (2017) 21–28.

[116] Y. Wang, D. Sun, Y. Yamada, S. Sato, Appl Catal A Gen 562 (2018) 11–18.

[117] A. Matsuda, Y. Matsumura, Y. Yamada, S. Sato, Molecular Catalysis 514 (2021) 111853.

[118] Y. Matsumura, A. Matsuda, Y. Yamada, S. Sato, Bull Chem Soc Jpn 94 (2021) 1651–1658.

[119] J. Huang, W.L. Dai, H. Li, K. Fan, J Catal 252 (2007) 69–76.

[120] D.W. Hwang, P. Kashinathan, J.M. Lee, J.H. Lee, U. hwang Lee, J.S. Hwang, Y.K. Hwang, J.S. Chang, Green Chem13 (2011) 1672–1675.

[121] B. Zhang, Y. Zhu, G. Ding, H. Zheng, Y. Li, Appl Catal A Gen 443–444 (2012) 191–201.

[122] H.P.R. Kannapu, Y.W. Suh, A. Narani, V. Vaddeboina, D.R. Burri, R.R. Kamaraju Seetha, RSC Adv 7 (2017) 35346–35356.

[123] H.P.R. Kannapu, Y.W. Suh, A. Narani, D.R. Burri, R.R. Kamaraju Seetha, Catal Letters 147 (2017) 90–101.

[124] Y.L. Zhu, J. Yang, G.Q. Dong, H.Y. Zheng, H.H. Zhang, H.W. Xiang, Y.W. Li, Appl Catal B 57 (2005) 183–190.

[125] J.T. Bhanushali, D. Prasad, K.N. Patil, K.S. Reddy, K.S. Rama Rao, A.H. Jadhav, B.M. Nagaraja, Int J Hydrogen Energy 45 (2020) 12874–12888.

[126] J. Zheng, J. Huang, X. Li, W.L. Dai, K. Fan, RSC Adv 2 (2012) 3801–3809.

[127] X. Li, J. Zheng, X. Yang, W. Dai, K. Fan, Chin J Catal 34 (2013) 1013–1019.

[128] S. Sato, R. Takahashi, T. Sodesawa, N. Honda, H. Shimizu, Catal Commun 4 (2003) 77–81.

[129] H. Gotoh, Y. Yamada, S. Sato, Appl Catal A Gen 377 (2010) 92–98.

[130] N. Ichikawa, S. Sato, R. Takahashi, T. Sodesawa, J Mol Catal A Chem 256 (2006) 106–112.

[131] F. Jing, B. Katryniok, M. Araque, R. Wojcieszak, M. Capron, S. Paul, M. Daturi, J.M. Clacens, F. De Campo, A. Liebens, F. Dumeignil, M. Pera-Titus, Catal Sci Technol 6 (2016) 5830–5840.

[132] J.H. Lee, S.B. Hong, Appl Catal B 280 (2021).

[133] H. Zhang, G.T. Lountos, C.B. Ching, R. Jiang, Appl Microbiol Biotechnol 88 (2010) 117–124.

[134] S. Sato, R. Takahashi, H. Fukuda, K. Inui, J Mol Catal A Chem 272 (2007) 164–168.

[135] Z. Zhong, H. Liu, R. Zhou, B. Ye, J. Fu, Z. Hou, ACS Sustain Chem Eng 11 (2023) 587–596.

[136] S.P. Adhikari, J. Zhang, Q. Guo, K.A. Unocic, L. Tao, Z. Li, Sustain Energy Fuels 4 (2020) 3904–3914.

[137] M. Affandy, C. Zhu, M. Swita, B. Hofstad, D. Cronin, R. Elander, V. Lebarbier Dagle, Fuel 333 (2023) 126328.

[138] T. Rajale, X. Yang, E.J. Judge, C.M. Moore, A. Martinez, M.F. Guo, K.K. Ramasamy, R. Elander, A.D. Sutton, Biofuels, Bioprod Biorefin 17 (2023) 1003–1011.

[139] H. Zhang, Y. Li, J. Zhuang, J. Dai, Z.-L. Xiu, C. Quan, Biotechnol Biofuels Bioprod 16 (2023) 94.

[140] D. Tinôco, S. Borschiver, P.L. Coutinho, D.M.G. Freire, Biofuels, Bioprod Biorefin 15 (2021) 357–376.

[141] Y. Zhang, D. Liu, Z. Chen, Biotechnol Biofuels 10 (2017) 299.

[142] P. Baral, V. Kumar, D. Agrawal, Crit Rev Biotechnol 42 (2022) 873–891.

[143] S.Y. Lee, H.U. Kim, Nat Biotechnol 33 (2015) 1061–1072.

[144] S. Van Dien, Curr Opin Biotechnol 24 (2013) 1061–1068.

[145] C.E. Nakamura, G.M. Whited, Curr Opin Biotechnol 14 (2003) 454–459.

[146] Y. Zhang, Z. Huang, C. Du, Y. Li, Z. Cao, Metab Eng 11 (2009) 101–106.

[147] V.E.T. Maervoet, M. De Mey, J. Beauprez, S. De Maeseneire, W.K. Soetaert, Org Process Res Dev 15 (2011) 189–202.

[148] E. Celińska, Crit Rev Biotechnol 32 (2012) 274–288.

[149] I.W. Bogorad, T.-S. Lin, J.C. Liao, Nature 502 (2013) 693–697.

[150] V. Guadalupe-Medina, H.W. Wisselink, M.A. Luttik, E. de Hulster, J.-M. Daran, J.T. Pronk, A.J. van Maris, Biotechnol Biofuels 6 (2013) 125.

[151] V. Kumar, S. Ashok, S. Park, Biotechnol Adv 31 (2013) 945–961.

[152] V. Kumar, S. Park, Biotechnol Adv 36 (2018) 150–167.

[153] M.J. Dunlop, Z.Y. Dossani, H.L. Szmidt, H.C. Chu, T.S. Lee, J.D. Keasling, M.Z. Hadi, A. Mukhopadhyay, Mol Syst Biol 7 (2011) 487.

[154] J. Haider, M.A. Qyyum, A. Hussain, M. Yasin, M. Lee, Biochem Eng J 140 (2018) 93–107.

[155] G.R. Harvianto, J. Haider, J. Hong, N. Van Duc Long, J.-J. Shim, M.H. Cho, W.K. Kim, M. Lee, Biotechnol Biofuels 11 (2018) 18.

[156] M. Goswami, S. Meena, S. Navatha, K.N. Prasanna Rani, A. Pandey, R.K. Sukumaran, R.B.N. Prasad, B.L.A. Prabhavathi Devi, Bioresour Technol 188 (2015) 99–102.

[157] https://www.basf.com/us/en/media/news-releases/2015/03/P-US-14-29.html.

[158] S. Adhikari, J. Zhang, K. Unocic, E.C. Wegener, P. Kunal, D.J. Deka, T. Toops, S. Sinha Majumdar, T.R. Krause, D. Liu, Z. Li, ACS Sustain Chem Eng 10 (2022) 1664–1674.

[159] A.A. Koutinas, B. Yepez, N. Kopsahelis, D.M.G. Freire, A.M. de Castro, S. Papanikolaou, I.K. Kookos, Bioresour Technol 204 (2016) 55–64.

[160] S. Gadkari, V. Narisetty, S.K. Maity, H. Manyar, K. Mohanty, R.B. Jeyakumar, K.K. Pant, V. Kumar, ACS Sustain Chem Eng 11 (2023) 8337–8349.

[161] G. Zang, A. Shah, C. Wan, Biofuels Bioprod Biorefin 14 (2020) 326–343.

[162] C. Ma, A. Wang, J. Qin, L. Li, X. Ai, T. Jiang, H. Tang, P. Xu, Appl Microbiol Biotechnol 82 (2009) 49–57.

[163] L. Zhang, J. Sun, Y. Hao, J. Zhu, J. Chu, D. Wei, Y. Shen, J Ind Microbiol Biotechnol 37 (2010) 857–862.

[164] X.-J. Ji, H. Huang, J.-G. Zhu, L.-J. Ren, Z.-K. Nie, J. Du, S. Li, Appl Microbiol Biotechnol 85 (2010) 1751–1758.

[165] K. Petrov, P. Petrova, Appl Microbiol Biotechnol 87 (2010) 943–949.

[166] T. Häßler, D. Schieder, R. Pfaller, M. Faulstich, V. Sieber, Bioresour Technol 124 (2012) 237–244.

[167] I.-M. Jurchescu, J. Hamann, X. Zhou, T. Ortmann, A. Kuenz, U. Prüße, S. Lang, Appl Microbiol Biotechnol 97 (2013) 6715–6723.

[168] L.J. Kim Borim, Lee Soojin, Park Joohong, Lu Mingshou, Kim Youngrok, J Microbiol Biotechnol 22 (2012) 1258–1263.

[169] D.-K. Kim, C. Rathnasingh, H. Song, H.J. Lee, D. Seung, Y.K. Chang, J Biosci Bioeng 116 (2013) 186–192.

[170] S.-J. Kim, S.-O. Seo, Y.-S. Jin, J.-H. Seo, Bioresour Technol 146 (2013) 274–281.

[171] T. Yang, Z. Rao, X. Zhang, M. Xu, Z. Xu, S.-T. Yang, PLoS One 8 (2013) e76149.

[172] X. Guo, C. Cao, Y. Wang, C. Li, M. Wu, Y. Chen, C. Zhang, H. Pei, D. Xiao, Biotechnol Biofuels 7 (2014) 44.

[173] S. Cho, T. Kim, H.M. Woo, J. Lee, Y. Kim, Y. Um, PLoS One 10 (2015) e0138109.

[174] J.-Y. Dai, P. Zhao, X.-L. Cheng, Z.-L. Xiu, Appl Biochem Biotechnol 175 (2015) 3014–3024.

[175] K. Jantama, P. Polyiam, P. Khunnonkwao, S. Chan, M. Sangproo, K. Khor, S.S. Jantama, S. Kanchanatawee, Metab Eng 30 (2015) 16–26.

[176] L. Li, K. Li, Y. Wang, C. Chen, Y. Xu, L. Zhang, B. Han, C. Gao, F. Tao, C. Ma, P. Xu, Metab Eng 28 (2015) 19–27.

[177] J. Fu, G. Huo, L. Feng, Y. Mao, Z. Wang, H. Ma, T. Chen, X. Zhao, Biotechnol Biofuels 9 (2016) 90.

[178] J.-W. Kim, J. Kim, S.-O. Seo, K.H. Kim, Y.-S. Jin, J.-H. Seo, Biotechnol Biofuels 9 (2016) 265.

[179] F. Xin, A. Basu, M.C. Weng, K.-L. Yang, J. He, Bioenergy Res 9 (2016) 15–22.

[180] Y.-G. Lee, J.-H. Seo, Biotechnol Biofuels 12 (2019) 204.

[181] S. Maina, E. Stylianou, E. Vogiatzi, A. Vlysidis, A. Mallouchos, G.-J.E. Nychas, A.M. de Castro, E. Dheskali, I.K. Kookos, A. Koutinas, Bioresour Technol 274 (2019) 343–352.

[182] C.W. Song, R. Chelladurai, J.M. Park, H. Song, J Ind Microbiol Biotechnol 47 (2020) 97–108.

[183] A.S. Afschar, K.H. Bellgardt, C.E. Vaz Rossell, A. Czok, K. Schaller, Appl Microbiol Biotechnol 34 (1991) 582–585.

[184] L.-H. Sun, X.-D. Wang, J.-Y. Dai, Z.-L. Xiu, Appl Microbiol Biotechnol 82 (2009) 847–852.

[185] A. Wang, Y. Xu, C. Ma, C. Gao, L. Li, Y. Wang, F. Tao, P. Xu, PLoS One 7 (2012) e40442.

[186] M.-Y. Jung, B.-S. Park, J. Lee, M.-K. Oh, Bioresour Technol 139 (2013) 21–27.

[187] L. Li, C. Chen, K. Li, Y. Wang, C. Gao, C. Ma, P. Xu, Appl Environ Microbiol 80 (2014) 6458–6464.

[188] A.M. Białkowska, E. Gromek, J. Krysiak, B. Sikora, H. Kalinowska, M. Jędrzejczak-Krzepkowska, C. Kubik, S. Lang, F. Schütt, M. Turkiewicz, J Ind Microbiol Biotechnol 42 (2015) 1609–1621.

[189] S. Cho, T. Kim, H.M. Woo, Y. Kim, J. Lee, Y. Um, Biotechnol Biofuels 8 (2015) 146.

[190] C. Zhang, W. Li, D. Wang, X. Guo, L. Ma, D. Xiao, Turk J Biol 40 (2016) 856–865.

[191] L. Dai, F. Tao, H. Tang, Y. Guo, Y. Shen, P. Xu, Metab Eng 44 (2017) 70–80.

[192] J. Yadagiri, V.S. Puppala, H.P.R. Kannapu, V. Vakati, K.S. Koppadi, D.R. Burri, S.R.R. Kamaraju, Catal Commun 101 (2017) 66–70.

[193] A. Takagaki, Catal Sci Technol 6 (2016) 791–799.
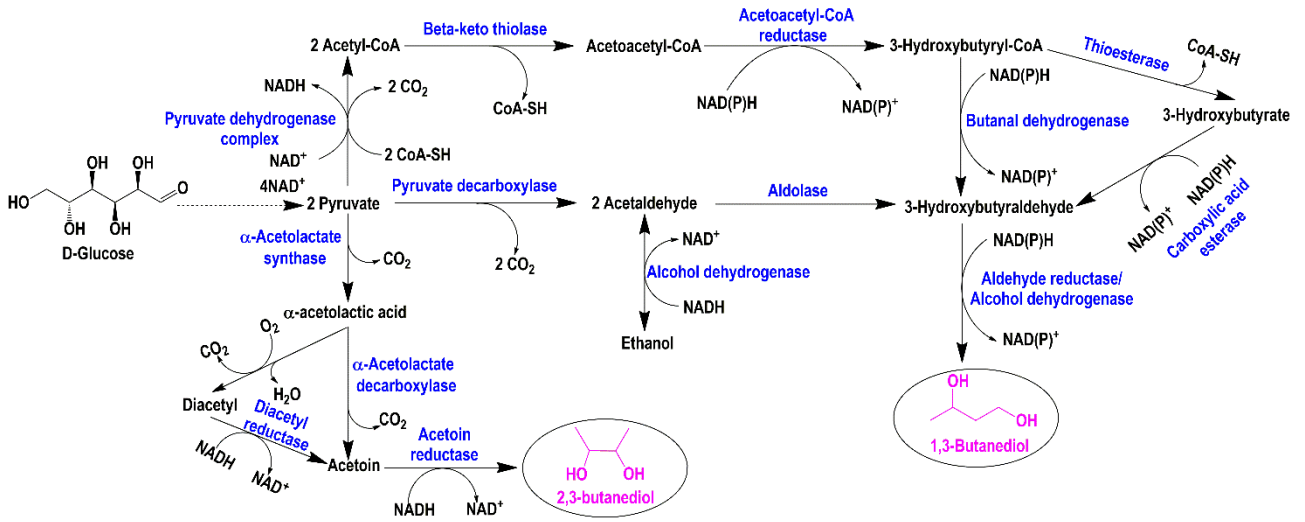
Fig. 1. Metabolic pathways for microbial synthesis of 2,3-BDO and 1,3-BDO [42].
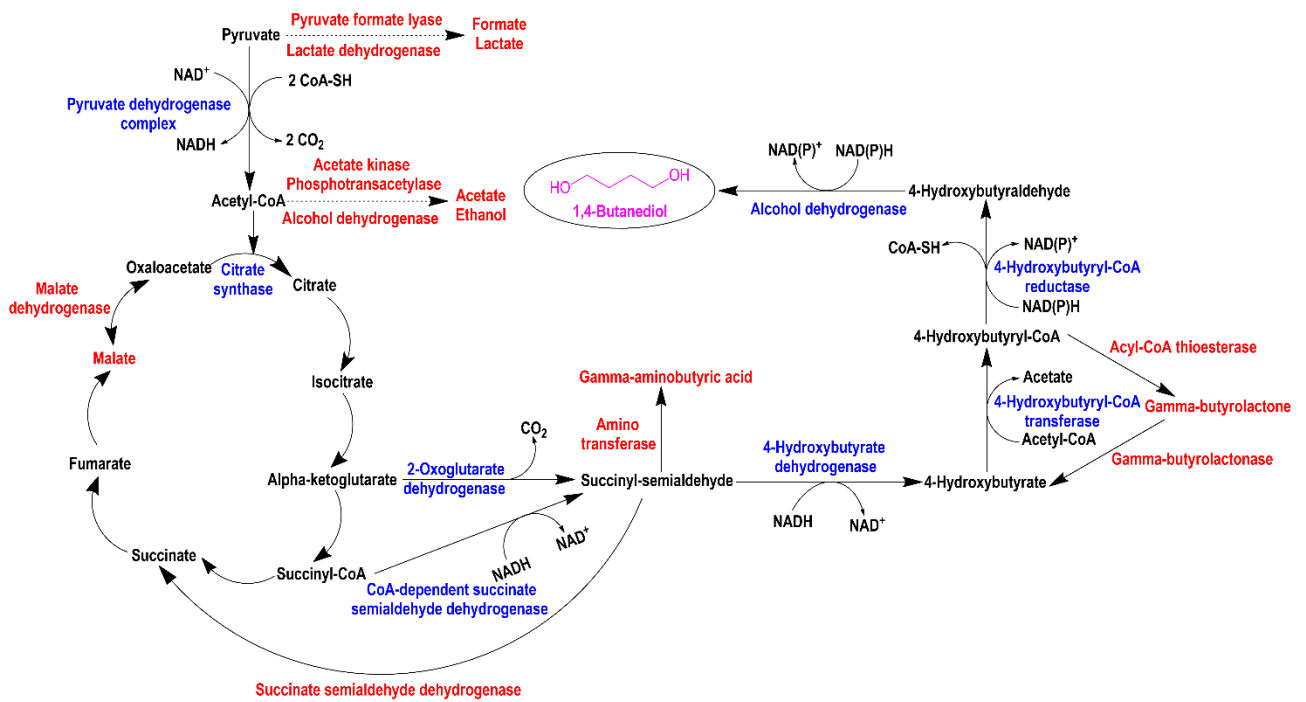
Fig. 2. Biochemical route for production of 1,4-BDO. The enzymes in red indicate the steps leading to carbon loss and by-product formation.
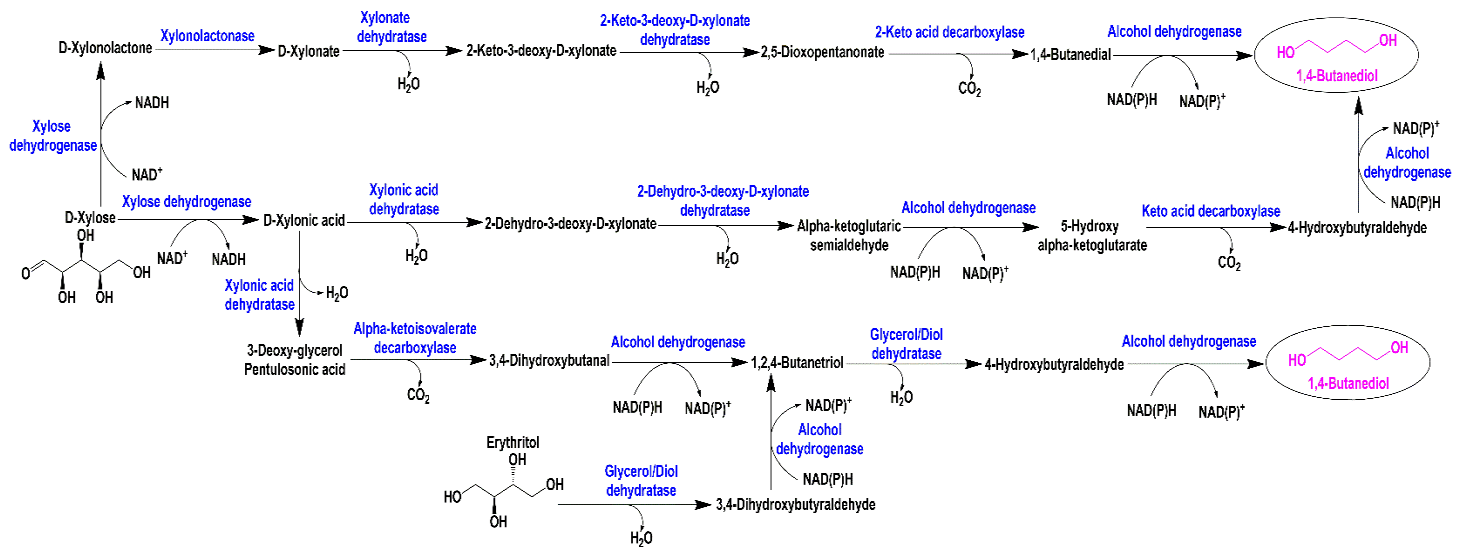
Fig. 3. Biochemical pathways for xylose and erythritol based production of 1,4-BDO.
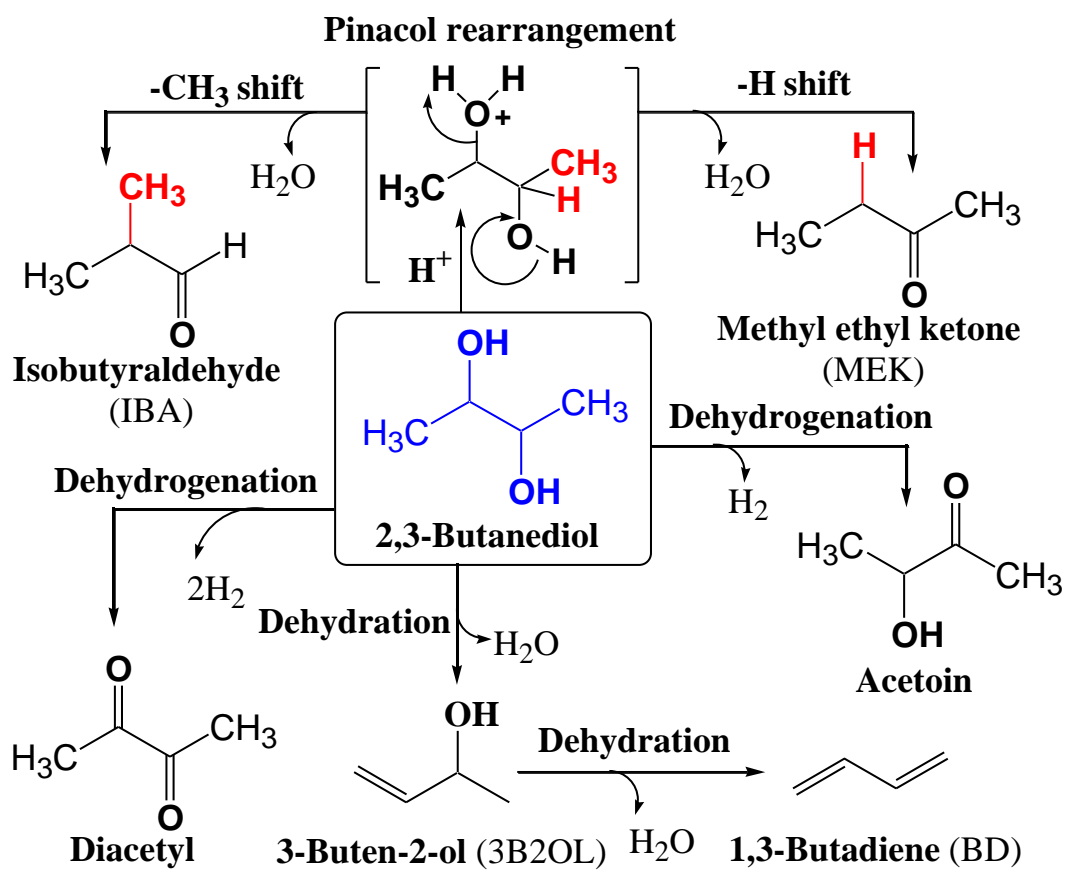
Fig. 4. Various derivatives of 2,3-BDO.
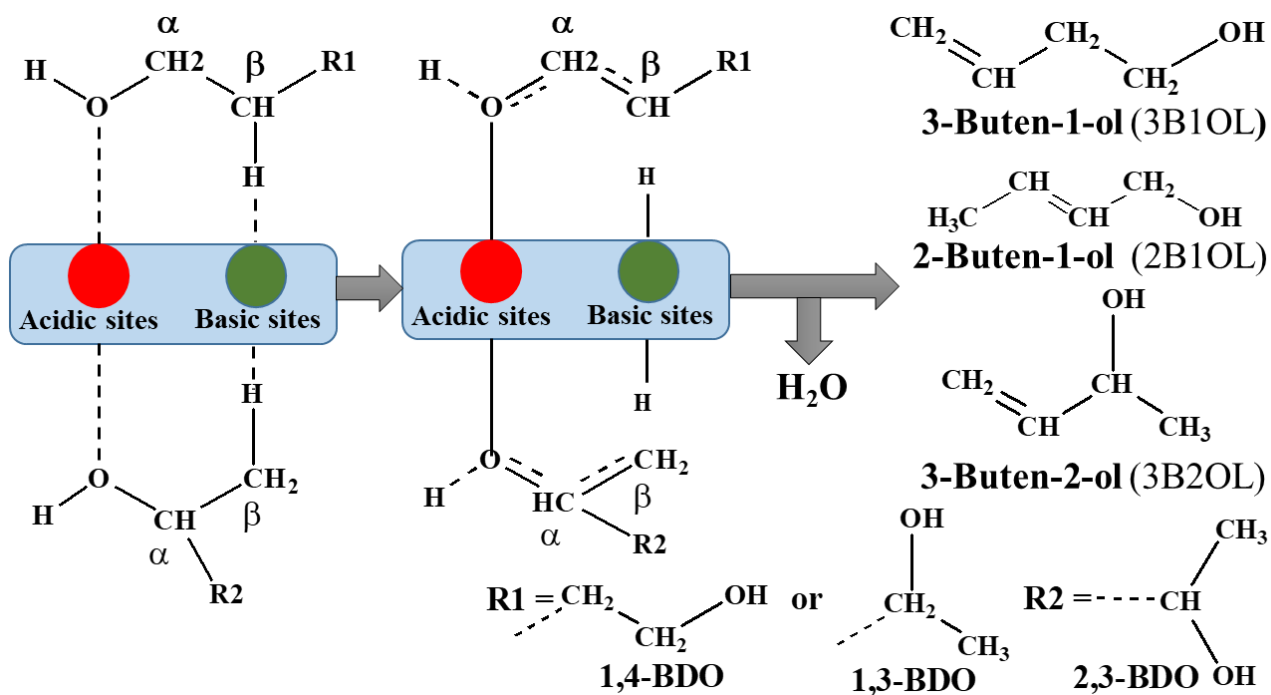
Fig. 5. Mechanism of BDOs dehydration to enol [97].
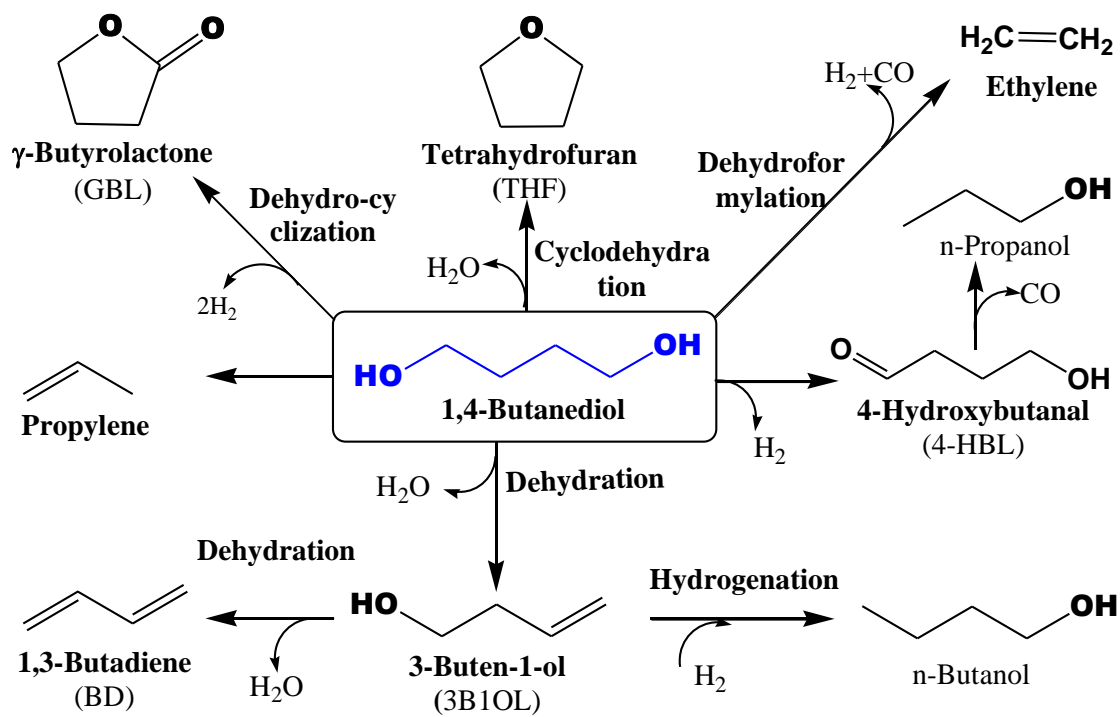
Fig. 6. Derivatives of 1,4-BDO.
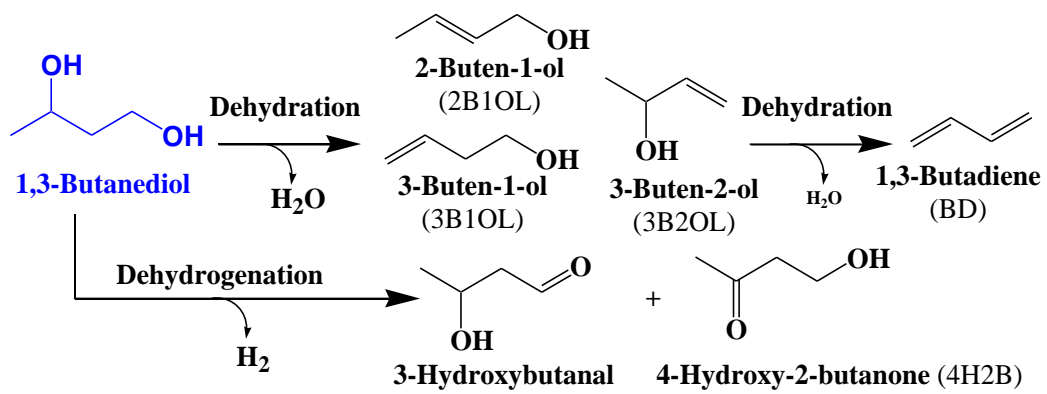
Fig. 7. Derivatives of 1,3-BDO.

Table 1: Properties of butanediols.
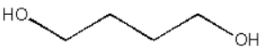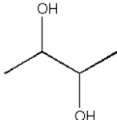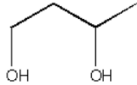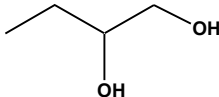
	1,4–BDO	2,3–BDO	1,3–BDO	1,2-BDO
Structure				
Molar mass, g/mol	90.12	90.12	90.12	90.12
Color	Colorless	Colorless	Colorless	Colorless
State @30 °C	Liquid	Liquid	Liquid	Liquid
Boiling point, °C	230	177	207	192
Melting point, °C	20.1	19	-77	-42
Density, g/cm^3	1.02	0.967	1.01	1.002
Water solubility	Miscible	Miscible	Miscible	Miscible
Vapor pressure, Pa	1.4@25 °C	23@20 °C	8@20 °C	2.7@20 °C
Heat Capacity (J/mol*K)	202.34 @298K	227.2 @300K	227.2 @300K	240.4 @298K

Table 2: Summary of high-level production of 2,3-BDO from pure and crude renewable carbon sources by wild type and engineered strains.

Microorganism	Genotype	Substrate	Fermentation mode	Titer (g/L)	Yield (g/g)	Productivity (g/L. h)	Ref.
Klebsiella pneumoniae	Wild type	Glucose	Fed-batch	150.0	0.48	3.95	[162]
Serratia marcescens	ΔswrW	Sucrose	Fed-batch	152.0	0.46	2.67	[163]
Klebsiella oxytoca	ΔaldA	Glucose	Fed-batch	130.0	0.48	1.63	[164]
Klebsiella pneumoniae	Wild type	Glycerol	Fed-batch	70.0	0.39	0.47	[165]
Paenibacilluspolymyxa	Wild type	Glucose	Fed-batch	111.0	-	2.06	[166]
Bacillus licheniformis	Wild type	Glucose	Fed-batch	144.7	0.40	1.14	[167]
Klebsiella pneumoniae	↑budA ↑budB	Glucose	Fed-batch	101.5	0.34	2.54	[168]
Klebsiella oxytoca	ΔldhA	Glucose	Fed-batch	115.0	0.41	2.27	[169]
Saccharomyces cerevisiae	Δpdc1Δpdc5, pointmutation in *mth1*, ↑alsS↑alsD↑bdh1	Glucose	Fed-batch	96.2	0.28	0.39	[170]
Bacillus amyloliquefaciens	↑bdh ↑gapA	Glucose	Fed-batch	132.5	0.45	2.95	[171]
Klebsiella pneumoniae	ΔadhEΔldhA	Glucose	Fed-batch	116	0.49	2.23	[172]
Klebsiella oxytoca	ΔbudC	Glucose	Fed-batch	142.5	0.42	1.47	[173]
Enterobacter cloacae	Mutant strain	Glucose	Fed-batch	110.9	0.39	1.98	[174]
Bacillus licheniformis	ΔbudC	Glucose	Fed-batch	123.7	-	2.95	[29]
Klebsiella oxytoca	ΔadhEΔackA-ptaΔldhAME	Glucose	Fed-batch	117.4	0.49	1.20	[175]
Enterobacter cloacae	ΔldhΔptsGΔbdhΔfrdA↑bdh↑galP	Glucose/Xylose	Fed-batch	152.0	0.49	3.50	[176]
Klebsiella oxytoca	ΔldhAΔpflBΔbudC↑bdh	Glucose	Fed-batch	106.7	0.40	3.10	[28]
Bacillus subtilis	↑alsS ↑alsD ↑budC ↑udhAΔuppΔacoAΔbdhAΔptaΔldh	Glucose	Fed-batch	103.7	0.49	0.46	[177]
Saccharomyces cerevisiae	ΔPDC ΔnoxE	Glucose	Fed-batch	154.3	0.40	1.98	[178]
*Klebsiella*sp.	Wild type	Sucrose	Fed-batch	119.4	0.40	1.84	[179]
Saccharomyces cerevisiae	↑alsS ↑alsD ↑BDH1 ↑noxE ΔADH ΔPDC	Glucose	Fed-batch	178.0	0.34	1.88	[180]
Enterobacterludwigii	Wild type	VHP Cane sugar	Fed-batch	111.0	0.40	1.11	[181]
Bacillus licheniformis	ΔbudC	Glucose	Fed-batch	123.0	0.41	1.71	[182]
Enterobacterludwigii	Random mutant	Xylose	Fed-batch	71.1	0.40	0.94	[27]
Enterobacterludwigii	Random mutant	Glucose	Fed-batch	144.5	0.47	1.51	[22]
Klebsiella oxytoca	Wild type	Molasses	Repeated batch	118.0	0.42	2.40	[183]

Organism	Strain	Substrate	Mode				Ref.
Klebsiella pneumoniae	Wild type	Jerusalem artichoke	Fed-batch/SSF	84.0	0.29	2.10	[184]
Enterobacter cloacae	Wild type	Cassava powder	Fed-batch/SSF	93.9	-	2.00	[185]
Enterobacter aerogenes	*ΔldhAΔscrR*	Sugarcane molasses	Fed-batch	98.7	0.37	2.74	[186]
Bacillus licheniformis	Wild type	Inulin	Fed-batch/SSF	103.0	-	3.43	[187]
Bacillus licheniformis	Wild type	Apple pomace	Fed-batch	113.0	0.49	0.69	[188]
Klebsiella oxytoca	*ΔpduCΔldhA*	Crude glycerol	Fed-batch	131.5	0.44	0.84	[189]
Enterobacter cloacae	Mutant strain	Sugarcane molasses	Fed-batch	90.8	0.36	1.66	[174]
Enterobacter cloacae	*ΔldhΔptsGΔbdhΔfrdA↑bdh↑galP*	Corn stover	Fed-batch	119.4	0.48	2.30	[176]
Enterobacter cloacae	Wild type	Xylose from corncob	Fed-batch	81.4	0.39	0.72	[190]
Saccharomyces cerevisiae	*↑alsS ↑alsD ↑BDH1 ↑noxE ΔADH ΔPDC*	Cassava	Fed-batch	132.0	0.32	1.92	[180]
Enterobacter ludwigii	Random mutant	Sugarcane bagasse	Fed-batch	63.5	0.36	0.84	[27]
Enterobacter ludwigii	Random mutant	Brewer's spent grains	Fed-batch	118.5	0.43	1.65	[25]
Enterobacter ludwigii	Random mutant	Bread waste	Fed-batch	138.8	0.48	1.45	[22]

ME: Metabolic evolution

Table 3: Summary of non-native 1,3-BDO production by microbial cell factories

Microorganism	Genotype	Substrate	Fermentation mode	Titer (g/L)	Yield (g/g)	Productivity (g/L. h)	Ref.
E. coli	↑*phaA*↑*phaB*↑*bld*	Glucose	Fed-batch	9.05	-	0.08	[40]
E. coli	↑*phaA*↑*phaB*↑*bld*	Glucose	Fed-batch	15.7	0.19	0.16	[41]
E. coli	↑*AKR*↑*DERA* ↑*PDC* Δ*adhE*Δ*ldhA*Δ*pflB*δ*yqhD*Δ*eutG*Δ*adhP*Δ*yjgB*Δ*ilvB*Δ*poxB*Δ*pta*	Glucose	Fed-batch	2.4	0.058	-	[43]
E. coli	↑*bld*[L273T]↑*yqhD*↑*phaA*↑*phaB*↑*pntA*↑*pntB*↑*sfp*↑*yqhD*	Glucose	Fed-batch	13.4	0.29	0.42	[36]
E. coli	↑*thl*↑*hbd*↑*tesB* ↑*car* ↓*fabD*↓*accABCD*	Glucose	Fed-batch	22.7	0.40	0.32	[42]
E. coli	↑*phaA*↑*phaB*↑*bld* ↑*yqhD*Δ*adhE*Δ*ldhA*Δ*poxB*Δ*pta-ackA*Δ*pyciA*	Glucose	Fed-batch	23.1	0.25	0.64	[44]
C. necator	↑*bld*↑*yqhD*↑*dra*↑*PDC* ↑*phaAB*Δ*phaC1*	CO_2	Fed-batch	3.0	0.39	0.025	[47]
Cell free *in vitro* synthesis	↑ADH ↑NOX ↑DERA ↑AKR ↑FDH	Ethanol	Batch	7.7	0.83*	0.16	[48]

*85% of theoretical yield

Table 4: Overview of 1,4-BDO production from different carbon sources by engineered microorganisms.

Microorganism	Genotype	Substrate	Fermentation mode	Titer (g/L)	Yield (g/g)	Productivity (g/L. h)	Ref.
E. coli	*ΔadhEΔpflBΔldhAΔmdhΔarcAΔlpdA* *Kp.lpdD354K gltAR163L↑sucCD↑sucD↑4hbd/↑sucA↑adh*(025B) *↑Cat2*	Glucose	Fed-batch	18.0	0.37	0.15	[18]
E. coli	-	Glucose	Fed-batch	29.0	0.25	0.60	[54]
E. coli	-	Glucose	Fed-batch	99.0	0.35	2.10	[54]
E. coli	-	Glucose	Fed-batch	>125.0	>0.40	>3.50	[51]
E. coli	*ΔxylAΔyjhHΔyagE↑xdh↑xylX↑mdlC*	Xylose	Batch	0.44	0.042	-	[60]
E. coli	*ΔxylAΔyagEΔyjhH↑xylB↑xylC↑xylD↑xylX↑kivd(V461I)↑yqhD*	Xylose	Fed-batch	9.2	0.22	0.26	[62]
E. coli	*ΔxylAΔyagEΔyjhH↑xylB↑xylC↑xylD↑xylX↑kivd(V461I)↑yqhD↑atoB↑mvaS↑mvaE*	Xylose	Fed-batch	12.0	0.26	0.40	[62]
E. coli	*↑araC↑araD↑araA↑araB↑araE↑kivd(V461I)↑yqhD*	Arabinose	Fed-batch	15.6	0.22	0.22	[62]
E. coli	*ΔgarLΔuxaC↑udh↑garD↑ycbC↑kivd(V461I)↑yqhD*	Galactouronic acid	Fed-batch	16.5	0.33	0.18	[62]
E. coli	*ΔxylAΔyagEΔyjhH↑xylBC↑xylD↑kivD↑yqhD↑ppdA-C-B* (S301AQ336AV300M)	Xylose		0.21	-	-	[61]
E. coli*	*↑gldABC*(S302AQ337A)	Erythritol	Batch	16.1	0.009	0.81	[191]
E. coli*	*↑pddABC*(S301AQ336A)	Erythritol	Batch	11.9	0.006	0.6	[191]
E. coli*	*↑gldABC*(S302AQ337A)	Erythritol	Batch	34.5	-	-	[63]

* The titer and productivities are in mg/L and mg/L. h, respectively.

Table 5: Literature review for vapor phase dehydration of 2,3-BDO to methyl ethyl ketone (MEK) in a fixed-bed reactor.

Catalyst	Acidity (µmol/g)	Reaction conditions			X (%)	Selectivity (%)				Ref.
		WHSV (h^{-1})	T (°C)	N_2 (ml/min)		MEK	BD	IBA	Others	
AIP	930	1.5	250	-	100	78.1	6.9	13.4	$C_8 – C_{12}$: 1.5	[74]
ZrP	840	400	250		11.2	65.8	3.5	23.5	$C_8 – C_{12}$: 4.1	
γ-Al_2O_3	189	10	250	25	82.8	73.3	3.2	2.8	$C_8 – C_{12}$: 19.9	[73]
H-BEA	220				81.6	51.9	4.6	16.3	$C_8 – C_{12}$: 26.1, 3B2OL: 0.2	
deAl BEA[1]	43	10	250	25	75.9	50.5	4.2	17.4	$C_8 – C_{12}$: 27.6, 3B2OL: 0.2	
Zr-BEA	270				80	25.7	2.3	7.2	$C_8 – C_{12}$: 63.1, 3B2OL: 0.1	
2% P/HZSM-5	1407	4	180	12.5	~100	~75	-	~15	-	[75]
1%B/HZSM-5	963.8	4	180	12.5	97.2	68.4	1.2	16.8	-	[71]
	963.8		200		100	69.7	1.4	20.1	-	
a-CP[2]	-	1780[3]	324.5	10	~100	~32	~20	5	3B2OL: ~16	[76]
P/SiO$_2$_9.8[4]	-	0.04	180	10	100	49.2	21.4	11.8	BT: 2.9	[77]

X: Conversion of 2,3-BDO, AIP: Aluminum phosphate, ZrP: Zirconium phosphate, BT: 1-Butene.

[1]Dealuminated BEA, [2]Ca/P = 1.3, [3]GHSV, [4]30 h time-on-stream.

Table 6: Literature review for vapor phase dehydration of 2,3-BDO to 3-buten-2-ol (3B2OL) in fixed-bed reactor.

Catalyst	Acidity	Basicity	Reaction conditions			X (%)	Selectivity (%)				Ref.
			WHSV (h⁻¹)	T (°C)	N_2 (ml/min)		3B2OL	MEK	IBA	Others	
ZrO_2 [1]	-	-	1	325	45[3]	62.5	48.6	16	1.3	IBO: 7.8, Acetoin: 14.9, Others: 11.4	[78]
ZrO_2 [2]	-	-			45	76.4	43.8	17.9	1.1	IBO: 7.4, Acetoin: 11.4, Others: 18.4	
CaO/ZrO_2 [1]	-	211.3[4]	1.06	350	80[3]	~60	~70	-	-		[80]
SrO/ZrO_2 [1]	-	-				~60	~78	-	-	-	
BaO/ZrO_2 [1]	-	-				~75	~75	-	-		
MgO/ZrO_2 [1]	-	-				~40	~70	-	-		
2K_P/SiO₂_20	30.2[6]	21.14[6]	1.2	400	100	64	78[5]	9		BTO: 10, Acetoin + BDOn: 2	[70]
1.75 Cs_P/SiO₂_20	24[6]	-				46	50[5]	10		BTO: 28.6, Acetoin + BDOn: 6	
1.82 Na_P/SiO₂–17.2[7]	18.15[6]	3.63[6]	1.11	180	100	94.6	53.7	17.4	1.5	BD: 13.5, Acetoin + BDOn: 1.9, BTO: 4.4	[77]
$3Sc_{0.5}Yb_{1.5}O_3$	-	-	1.06	411	45[3]	99.2	35.3	14.9	6.3	BD: 9.2, IBO: 5.9, Others: 28.4	[67]
Nd_2O_3	-	-		425		87.8	35.2	16.9	4.0	BD: 0.0, IBO: 6.0, Others: 37.9	

Acidity: NH_3 desorbed $\times 10^7$ mol min⁻¹ g⁻¹, Basicity: CO_2 desorbed $\times 10^7$ mol min⁻¹ g⁻¹, X: Conversion of 2,3-BDO, IBO: 2-Methyl-1-propanol, BDOn: Butadiene (diacetyl), BTO: 2,3-Epoxybutane.
[1]Monoclinic structure, calcined at 800 °C, [2]Tetragonal structure, calcined at 800 °C, [3]Hydrogen, [4]Unit of NH_3 µmol/g (from [79]), [5]Combined selectivity of BD and 3B2OL, [6]Values are rounded off to nearest integer, [7]After 10 h time-on-stream.

Table 7: Literature review for vapor phase dehydration of 2,3-BDO to 1,3-butadiene (BD) in fixed-bed reactor.

Catalyst	Acidity (mmol/g)	Basicity (mmol/g)	WHSV (h^{-1})	T (°C)	N_2 (ml/min)	X (%)	BD	MEK	IBA	Others	Ref.
Sc_2O_3	-	-		411		100	88.3	1.1	0.1	3B2OL: 0.8, IBO: 0.3, Others: 9.4	[67]
Lu_2O_3	-	-	1.06	425	45[1]	99	23.2	23.1	1.8	3B2OL: 5.0, IBO: 0.8, Others: 46.1	
CeO_2	-	-		425		100	0.5	39.2	2.4	3B2OL: 0.5, IBO: 0.6, Others: 56.8	
γ-Al_2O_3	0.24	0.059	11.8	450	100	100	28	56.9	3.3	C_3: 1.4, Others: 10.4	[84]
			395	350	-[2]	13	60	11	13	BTO: 15	[83]
$GdPO_4$	-	-				100	~50	~38	~12	-	
$NdPO_4$	-	-	30[3]	300	100	100	~55	~35	~10	-	[85]
$LaPO_4$	-	-				~95	~50	~ 40	~9	-	
$2K\_P/SiO_2\_20$	30.2[6]	21.14[6]				64	78[4]	9[5]		BDOn + Actn: 2 BTO: 10	[70]
			1.2	400	100						
$1.5Cs\_P/SiO_2\_20$	-	-				83	50	12		BDOn + Actn: 4 BTO: 7.3	
$10\%CsH_2PO_4/CARiACT$ Q10	-	-	0.99	404	30	>99.9	91.9	7.0	0.3	3B2OL: 0.2, Butenes: 0.4, Others: 0.2	[86]

X: Conversion of 2,3-BDO, IBO: 2-Methyl-1-propanol, BTO: 2,3-Epoxybutane, Actn: Acetoin.

[1]Hydrogen, [2]Argon, [3]Value is in gcata·h·mol^{-1}, [4]Sum of BD and 3B2OL selectivity, [5]Sum of MEK and IBA selectivity, [6]Values are rounded off to nearest integer, and unit is NH_3 desorbed×10^7 mol min^{-1} g^{-1}.

Table 8: Literature review for vapor phase dehydration of 2,3-BDO to acetoin in a fixed-bed reactor.

Catalyst	Reaction conditions			X (%)	Selectivity (%)			Ref.
	WHSV (h^{-1})	T (°C)	N_2 (ml/min)		Acetoin	BDOn	Others	
20Cu-SiO_2-10.5	60	280	40	76	94.5	-	-	[87]
15Cu-Al_2O_3	2.5	220	100	98	49	9	42	[88]
15Cu-ZrO_2				97	75	15	10	
15Cu-Al_2O_3[1]	2.5	220	100	89	39	-	69	[88]
15Cu-ZrO_2[1]	2.5	220	100	85	89	-	11	[88]
Zn-Cr oxide	1.6[2]	375	-	70	~50	~40	-	[89]
Mg-V oxide	1[2]	350	1[3]	89	26	62.3	-	

X: Conversion of 2,3-BDO, BDOn: Butanedione (Diacetyl).

[1]Hydrogen was used in the feed, H_2/2,3-BDO mole ratio: 10, [2]LHSV, [3]Oxygen, 2,3-BDO/O_2 mole ratio: 1.

Table 9: Literature review for vapor phase conversion of 2,3-BDO to butylenes in a fixed-bed reactor.

Catalyst	Reaction conditions			X (%)	Selectivity (%)				Ref.
	WHSV (h^{-1})	T (°C)	H_2 (ml/min)		Butylene	MEK	IBA	Others	
9.2%CuO/ZSM-5(280)	3.0	250	5[1]	100	62.84	24.3		Olefines: 2.83	[92]
5V/SiO$_2$	1.5	500	40[2]	100	~45	~30	~15	C_1-C_3: ~5, Others: 5	[94]
Cu – PMFI	1	250	94.8 kPa	96	65	21	-	Pentene: 6.6, Hexenes: 3.0, Others: 4.4	[90]
Cu/Al-MCM-48 (100)					72.6	10.1	0.4	16.9	
Cu/Al-SBA-15 (50)	3.0	250	5[1]	100	76.6	4.3	0.2	18.9	[91]
Cu/meso-ZSM5 (280)					40.3	1.7		58	

X: Conversion of 2,3-BDO, PMFI: Pillared MFI type zeolite.

[1]H_2/2,3-BDO (mole ratio): 5:1, [2]Nitrogen.

Table 10: Literature review for 1,4-BDO dehydration to tetrahydrofuran (THF).

Catalysts	Acidity	Reaction conditions			X (%)	Selectivity (%)		Ref.
		WHSV (h^{-1})	T (°C)	N_2 (ml/min)		THF	Others	
Fixed-bed reactor								
2.5 wt% Yb_2O_3/ZrO_2	98.2	53.7	310	30	-	~80	BTO: ~20	[97]
m-ZrO_2	114.5				-	~78	BTO: ~22	
Al_2O_3	-	2.4	325	26	100	97.4	3B1OL: 0.1, Others: 2.5	[112]
t-ZrO_2	-				99.9	96.8	3B1OL: 0.7, GBL: 0.3, Others: 2.3	
Yb/SiO_2	-				100	98.3	3B1OL: 0.2, GBL: 0.1, Others: 1.4	
Yb/t-ZrO_2	-				77.1	50.7	3B1OL: 39.4, GBL: 0.8, Others: 9.1	
AMW	-	1.0	375	30	97	99	Others: 1	[192]
CaO-ZrO_2[1]	261	1.02	350	30	99.1	79.6	3B1OL: 18.1, GBL: 1.1, Others: 1.2	[107]
Batch reactor								
Amberlyst-15	-	100 °C, 900 ml pure 1,4-BDO, 5 g catalyst, 1 h			29.32, 45.7[2]	Selective[3]	1%	[96]
Bu_4PBr	-	220 °C, 0.04 ml 1,4-BDO, 0.58 g of catalyst, 15 min			100	72%	BD: 27, Butanal: 1	[114]
$HnbMoO_6$	1.9[4]	140 °C, 3 ml water solvent, 900 ml 1,4-BDO, 0.05 g catalyst, 3 h			19	>99	<1%	[193]
HZSM-5	200				50	>99	<1%	
HZSM-5 (23)	-	225 °C, 17 bar N_2, 1,4-dioxane solvent, 0.7 mol 1,4-BDO/L, 10 g catalyst, 3 h			93.8	99.6	<1%	[99]
H-Y (5.1)	-				89.5	99.3		
H-Mordenite (90)	-				88.2	99.7		
H-Beta (25)	-				90.3	99.9		
Ferrierite (20)	-				80.2	99.5		
4.6CuO/nano ZSM-5	-	170 °C, 2.5 g catalyst, 50 g 1,4-BDO, 3 h			100	>99	<1%	[100]

X: Conversion of 1,4-BDO, Acidity: μmol NH_3/g, AMW: Activated marble waste,
[1]Calcined at 500 °C, [2]Conversion at 50 min using reactive distillation, [3]Selectivity is regarded as very high, [4]Determined by P MASNMR.

Table 11: Literature review for vapor phase dehydration of 1,4-BDO to 3-buten-1-ol (3B1OL) in a fixed-bed reactor.

Catalyst	Acidity	Basicity	WHSV (h^{-1})	T (°C)	N_2 (ml/min)	X (%)	3B1OL	THF	GBL	Others	Ref.
ZrO_2	-	-	6	350	73[1]	86.4	48.0	44.9	-	7.1	[103]
1.5 Na-ZrO_2	0	396				18.7	71.8	20.8	2.1	5.3	
1.5 Li-ZrO_2	-	-	1.8	325	73[1]	19.1	63.5	27.9	1.0	7.5	[104]
1.5 K-ZrO_2	-	-				19.0	63.6	26.9	3.9	5.6	
1.5 wt% P/ZrO_2	142	103				99.9	11.4	80.6	0.6	7.4	
CaO/ZrO_2	295	496				92.6	65.4	11.3	-	23.3	
SrO/ZrO_2	127	211	3.3	350	30	84.1	45.1	33.7	-	21.2	[105]
BaO/ZrO_2	72	164				74.3	35.9	40.8	-	23.3	
12.5 wt% CaO/ZrO_2 [2]	251	486	1.02	350	30	94.6	68.9	9.8	6.3	15	[107]
CeO_2	-	-	0.1662	400	73 [1]	87.6	68.1	3.7	-	BD: 1.7, Others: 26.5	[40]
CeO_2	-	-	0.073	425	29 [1]	74	57.1	17.4	3.0	2B1OL: 7.5, Others: 15	[108]
CeO_2 – N	-	-				78.5	55.0	3.3	2.4	39.2	
CeO_2 – AH	-	-	1.02[3]	375	-	91.7	51.4	4.2	3.1	41.3	[111]
CeO_2	-	-				94.5	63.2	3.0	0.9	32.9	
Yb/ZrO_2	281[4]	281[4]	2.5	325	26	50.8	86.5	4.3	1.1	8.1	[112]
Yb_2O_3	-	-	22.17	375	30	33.9	87.6	1.3	0.9	2B1OL: 7.5	[82]
Sc_2O_3						20.6	70	22.8	1.7	2B1OL: 1.5	
Mg_7Yb_3 oxide	116	260.5	1.08	350	-	90.4	78.6	-	-	21.7	[113]

X: Conversion of 1,4-BDO, Acidity: µmol NH_3/g, Basicity: µmol CO_2/g.

[1]mmol/h of He, [2]Sample is calcined at 650 °C, [3]LHSV, [4]Values of acidity and basicity are for 10 wt% Yb loading on monoclinic ZrO_2.

Table 12: Literature review for vapor phase dehydration of 1,4-BDO to 1,3-butadiene (BD).

Catalyst	Reaction Conditions			X (%)	Selectivity (%)		Ref.
	WHSV (h^{-1})	T (°C)	N_2 (ml/min)		BD	Others	
CeO$_2$		275	29[1]	6.3	87.4	Others: 12.6	
	6	450		94.9	24.8	3B1OL: 25.9, THF: 7.6, Others: 41.7	
SiO$_2$-Al$_2$O$_3$	9	200		26.6	67.2	THF: 32.8	[109]
		275	29[1]	99.7	5.0	THF: 92.3, Others: 2.7	
	6	425		99.8	2.7	THF: 92.6, 3B1OL: 0.1, Others: 4.6	
γ-Al$_2$O$_3$	9	200		17.3	69.5	THF: 30.5	
		275	29[1]	100	0.2	THF: 99.3, Others: 0.5	
		425		100	3.1	THF: 91.8, Others: 5.1	
Y$_2$Zr$_2$O$_7$	0.31	375	30	100	58.8	3B1OL: 23.8, 2B1OL: 4.4, THF: 3.7, GBL: 0.1, Propylene: 5.8, Others: 3.4	[117]
Dy$_2$Zr$_2$O$_7$				99.8	66.4	3B1OL: 20.6, 2B1OL: 4.7, THF: 3.0, 3GBL: 0.1, Propylene: 1.8, Others: 3.4	
Yb$_2$O$_3$	21.74	360	30	100	96.6	Propylene: 0.7, THF: 0.1, Others: 2.5	[116]
Bu$_4$PBr[2]	220 °C, N_2, 0.5 mmol n-hexane, 0.05 mmol HBr, 0.5 mmol 1,4-BDO, 1.7 mmol catalyst, 2 h			100	94	THF: 5, Butanal: 1	[114]

X: Conversion of 1,4-BDO.
[1]Helium, [2]Reaction was performed in glass vial in nitrogen atmosphere.

Table 13: Literature review for the conversion of 1,4-BDO to γ-butyrolactone (GBL) in a fixed-bed reactor

Catalyst	Reaction Conditions				X (%)	GBL selectivity (%)	Ref.
	WHSV (h^{-1})	T (°C)	N_2 (ml/min)	H_2 (ml/min)			
Cu(12)/SiO$_2$					86.7	95.8	
Na(1)-Ca(7)-Cu(12)/SiO$_2$	2	250	45	17	97.0	93.6	[120]
Cu(80)/SiO$_2$					98.6[1]	99	
Cu-Ba/SiO$_2$					~100	~100	
Cu-Ca/SiO$_2$	1	260	-	5[2]	~100	~98	[121]
Cu-Sr/SiO$_2$					~100	~98	
Cu/SiO$_2$					~99	~99	
Cu/MgO	2	250	18	-	~60	~99	[122]
Cu/MgO-Al$_2$O$_3$					~15	~99	
Cu-Zn-Al	0.06	210	-	125[3]	100	98.6 [6]	[124]
10Co$_3$O$_4$-20Cu-70MgO					~83	~95	
10Cr$_2$O$_3$-20Cu-70MgO	2	~200	-	40	~70	~80	[123]
1ZnO-20Cu-79MgO					~75	~95	
10Cu/CeO$_2$-Al$_2$O$_3$	-	260	-	30	100	98	[125]
3Au/TiO$_2$[4]	140 °C, 1.25 MPa[5], TBP solvent, 0.069 ml 1,4-BDO/ml of solvent, 8 h reaction.				99	100	[119]
3Au/SnO$_2$[4]	140 °C, 1.2 MPa[5], TBP solvent, 0.080 ml 1,4-BDO/ml of solvent, 2 h.				94	59	[127]
5Au/SnO$_2$[4]					53	83	

X: Conversion of 1,4-BDO, TBP: Tributyl phosphate.

[1]Reaction was performed without hydrogen, [2]H_2/1,4-BDO: 5 (mol ratio), [3]H_2/1,4-BDO: 125 (mol ratio), [4]Reaction was performed in batch reactor, [5]Batch reactor was pressurized using air, [6]n-Butanol: 0.9%, others: 0.5%.

Table 14: Conversion of 1,3-BDO to unsaturated alcohols (UOL) and 1,3-butadiene (BD) in a fixed-bed reactor.

Catalysts	Reaction conditions			X (%)	Selectivity (%)			Ref.
	WHSV (h^{-1})	T (°C)	N_2 (ml/min)		UOL	BD	Others	
CeO_2[1]	13.2	325	73[2]	61.0	97.7	-	2.3[3]	[128]
Fe(III)-CeO_2				44.1	98.6	-	1.4[3]	
Co(II)-CeO_2				54.1	97.8	-	2.2[3]	
Ni(II)-CeO_2				69.0	96.5	-	3.5[3]	
Yb_2O_3	6.7	325	20	33.4	87.3	-	4.2	[129]
Y_2O_3				33.5	85.9	-	8.3	
Pr_6O_{11}				4.4[4]	12.1	-	40.3	
Sm_2O_3				3.1[4]	16.6	-	33.9	
ZrO_2	11.4	325	30	25.3	60.9	0	39.4	[130]
		375		71.4	41.7	3.9	54.4	
Yb_2O_3-ZrO_2 - 800	7.35	200	30	83.9	94.7	-	5.3[5]	[118]
ZSM-5 (260)	14.1	300	60[6]	>95	1Bol: 1.0, 2Bol: 0.3, 3B1OL: 8.7, 3B2OL: 2.3	60	Propylene: 24, MEK: 1.8, MVK: 1.3	[131]
Al-SBA-15 (102)				>95	1Bol: 1.1, 2Bol: 2.2, 3B1OL: 0.6	53	Propylene: 39, MEK: 2.1, MVK: 0.1	
H-FER (130)	1.39	300	50	100	3B1OL: ~10	~60	Propylene: ~20 MEK: ~10	[132]

X: Conversion of 1,3-BDO, MVK: Methyl vinyl ketone, 1Bol: 1-butanol, 2Bol: 2-Butanol.

[1]Catalyst was prepared by amorphous citrate method, [2]mmol/h, [3]3-Buten-2-one is the major by-product with small amount of BD, [4]Conversion was low due to high basicity of REO, [5]Selectivity to MEK and MVK, [6]Hellium.

Table 15: Literature review on dehydrogenation of 1,3-BDO.

Catalyst	Reaction conditions			X (%)	Selectivity (%)				Ref.
	WHSV (h^{-1})	T (°C)	N$_2$ (ml/min)		4H2B	MEK	AcH	AcMe	
CuO				40.8	55.9	6.1	2.7	17.8	
Cu/ZnO				66.3	55.5	19.9	1.7	9.2	
Cu/Al$_2$O$_3$	28.3	240	30[1]	98.4	2.6	51.5	3.6	15.5	[134]
CuO/ZrO$_2$				99.4	7.1	50.1	3.9	19.6	
Cu/MgO				89.8	22.8	22.0	7.3	28.6	
PtSb$_2$/AC[2]	70 °C, 2MPa O$_2$, aq. 1,3-BDO (10g/L), 0.2g catalyst, 14 h.			95.5	82.3[3]	3-HBAD: 0.3, 2-BA: 6.7, 4-HYBO: 5.7, Others: 5.0			[135]

X: Conversion of 1,3-BDO, AcH: Ethanal, AcMe: Propanone, 3-HBAD: 3-Hydroxybutyraldehyde, 2BA: 2-Butenal, 4HYBO: 4-Hydroxy-2-butanone.

[1]Hellium, [2]Reaction was performed in batch reactor, [3]3-Hudroxybutyric acid (3-HBA) was a major product.